Electronic Supplementary Information

Supramolecular network-based artificial light-harvesting system employing an AIE-active metallacycle for aqueous-phase photocatalytic oxidation

Ni Mao,[a] Ponmani Jeyakkumar,[a] Qian Liu,[a] Xiaorong Hou,[a] Xueqi Tian,[b] Huilan Yue,[c] Xiujun Yu[d] and Xiao-Yu Hu*[a,b,c]*

[a]College of Materials Science and Technology, Nanjing University of Aeronautics and Astronautics, Nanjing 211106, P. R. China

[b]College of Chemistry and Materials, Jiangxi Normal University, Nanchang 330022, P. R. China

[c]Qinghai Provincial Key Laboratory of Tibetan Medicine Research, Northwest Institute of Plateau Biology, Chinese Academy of Sciences, Xining 810008, P. R. China

[d]College of Chemistry and Environmental Engineering, Shenzhen University, Shenzhen 518060, P. R. China

**Corresponding Author: tianxq@jxnu.edu.cn; huxy@nuaa.edu.cn*

Table of Contents

1. General information

The commercially available reagents and solvents were either employed as purchased or dried according to procedures described in the literatures. All reactions were performed under nitrogen atmosphere unless otherwise stated. Analytical thin layer chromatography (TLC) was performed using 0.25 mm silica gel plates. Column chromatography was performed with silica gel (200-300 mesh) produced by Shanghai Titan Scientific Co., Ltd. All yields were given as isolated yields. NMR spectra (^{1}H NMR, ^{13}C NMR, ^{31}P NMR, and 2D NMR) were recorded on a Bruker Avance 400 MHz spectrometer at room temperature, with tetramethylsilane (TMS) as internal standard and solvent signals as internal references. Chemical shifts (δ) are reported in parts per million (ppm). Multiplicities were abbreviated as follows: d = doublet, t = triplet, q = quartet, m = multiplet, and coupling constant (*J*) in Hertz (Hz). High-resolution electrospray ionization mass spectra (HR-ESI-MS) were recorded on an Orbitrap Exploris 120 equipped with an electrospray ionization (ESI) probe operating in positive-ion mode with direct infusion. UV-visible spectra were recorded with a Shimadzu UV 1780 UV-Vis Spectrophotometer. Scanning electron microscope (SEM) investigations were carried out using a FEI Quanta FEG 250 instrument. Fluorescence spectra were recorded on a FLS980 fluorescence spectrophotometer (Edinburg Instruments Ltd., Livingstone, UK). The fluorescence lifetimes were measured by time-correlated single photon counting on a FLS980 instrument equipped with a pulsed xenon lamp. The quantum yields were carried out on a FLS980 instrument with the integrating sphere. Dynamic light scattering (DLS) measurements were carried out on a Malvern Zetasizer Prosystem. The mass spectra of self-assembled metallacycle **PyCEPt-1** and **PyPt-1** were recorded on a SYNAPT G2si MS/MS mass spectrometer using electrospray ionization with a MassLynx operating system. Compounds **H-7**[1] and **G-1**[2] were synthesized according to the reported procedures.

2. Synthetic procedures and characterization data

Synthesis of ligand PyCE

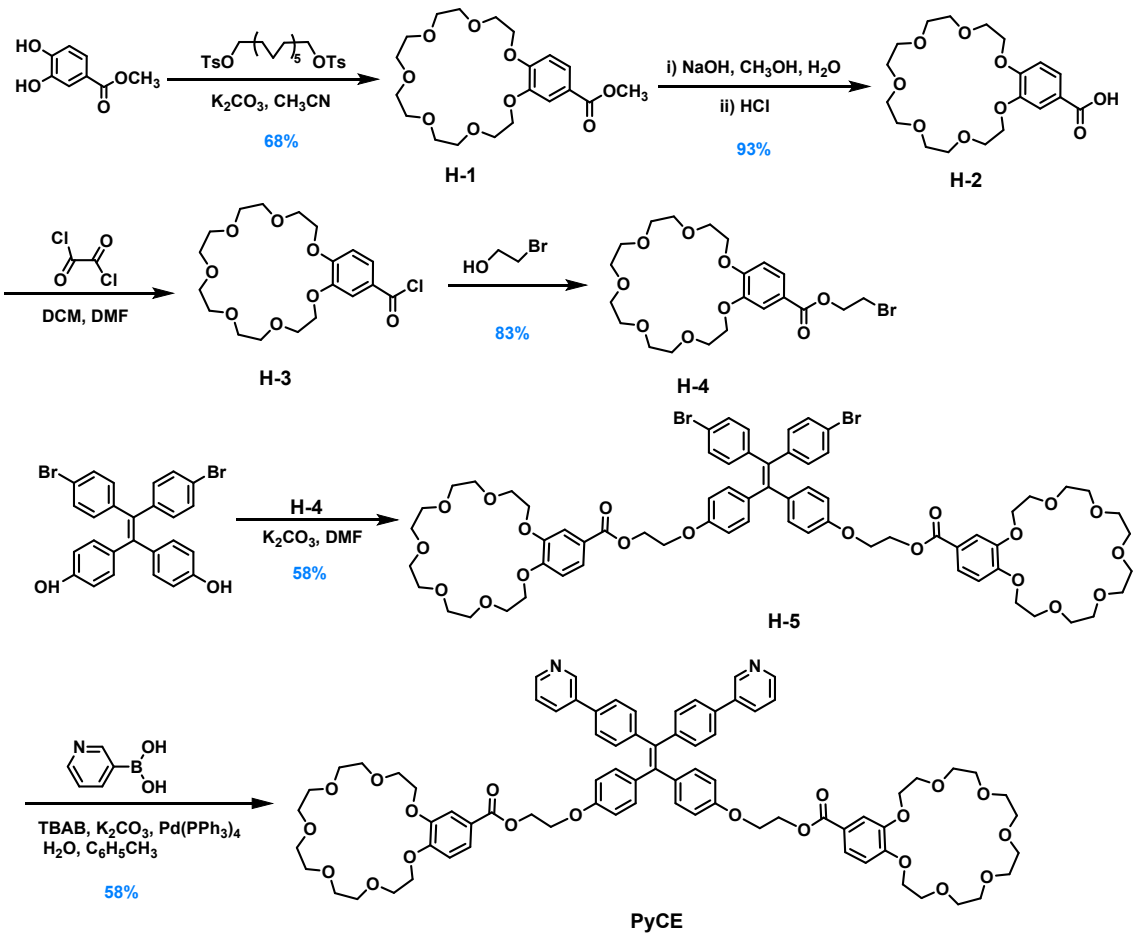

Scheme S1 Synthesis route of host molecule **PyCE**.

Synthesis of compound **H-1**[3]

Under a nitrogen atmosphere, methyl 3,4-dihydroxybenzoate (2.55 g, 15 mmol), hexaethylene glycol bis(*p*-toluenesulfonate) (8.86 g, 15 mmol), and K_2CO_3 (8.28 g, 60 mmol) were added to a reaction flask. CH_3CN was then introduced to dissolve the mixture under stirring, and the resulting solution was heated at 75°C for 12 hours. After completion of the reaction, the solvent was removed under reduced pressure, and the crude product was purified by silica gel column chromatography (DCM/CH_3OH = 100:1, *v*/*v*) to afford compound **H-1** as a yellow oil (4.24 g, 10.23 mmol, yield: 68%). ^1H NMR (400 MHz, $CDCl_3$, 298 K) δ 7.65 (d, J = 8.4 Hz, 1H), 7.54 (s, 1H), 6.87 (d, J = 8.4 Hz, 1H), 4.23 – 4.18 (m, 4H), 3.98 – 3.91 (m, 4H), 3.88 (s, 3H), 3.85 – 3.78 (m, 4H), 3.76 – 3.72 (m, 4H), 3.68 (s, 8H).

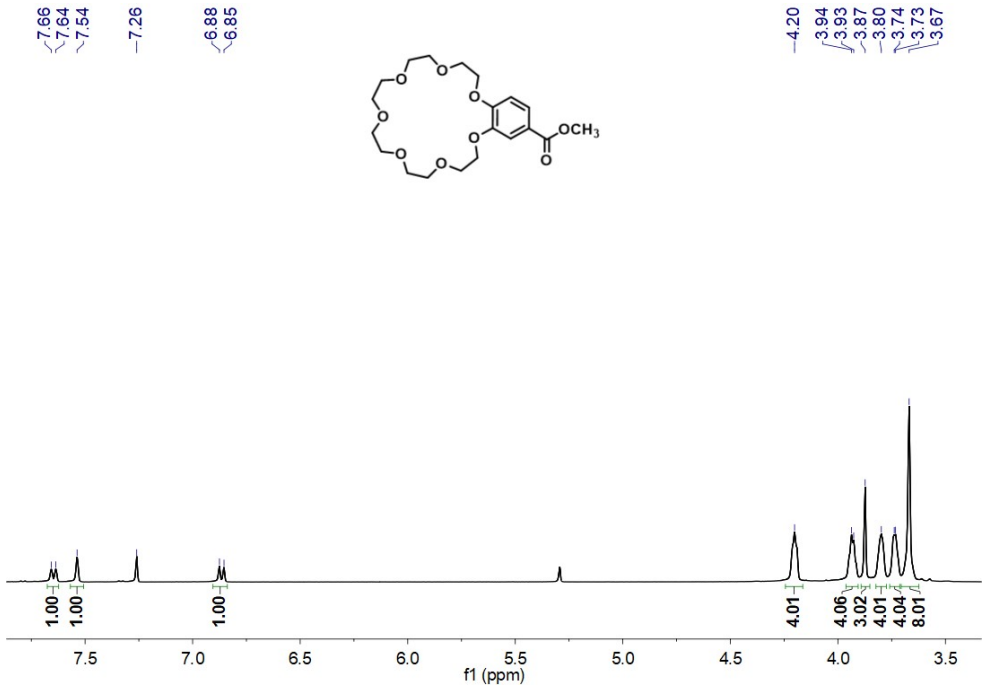

Fig. S1 ^{1}H NMR spectrum (400 MHz, $CDCl_3$, 298 K) of compound **H-1**.

Synthesis of compound **H-2**[4]

Compound **H-1** (5 g, 12.10 mmol) and NaOH (2.40 g, 60 mmol) were added to a reaction flask, H_2O (20 mL) and CH_3OH (100 mL) were then added as solvents, and the mixture was stirred until complete dissolution. The reaction solution was heated to 50°C and maintained for 5 hours. After completion, the system was cooled to room temperature, diluted with H_2O (100 mL), and adjusted to pH = 3 using HCl. Extraction was performed three times with DCM, and the combined organic phases were processed to afford compound **H-2** as a white powder (4.52 g, 11.29 mmol, yield: 93%). ^{1}H NMR (400 MHz, DMSO-d_6, 298 K) δ 12.64 (s, 1H), 7.54 (d, J = 7.2 Hz, 1H), 7.44 (s, 1H), 7.05 (d, J = 8.5 Hz, 1H), 4.14 (dd, J = 14.6, 3.9 Hz, 4H), 3.79 – 3.75 (m, 4H), 3.63 – 3.59 (m, 4H), 3.57 – 3.53 (m, 4H), 3.51 (s, 8H).

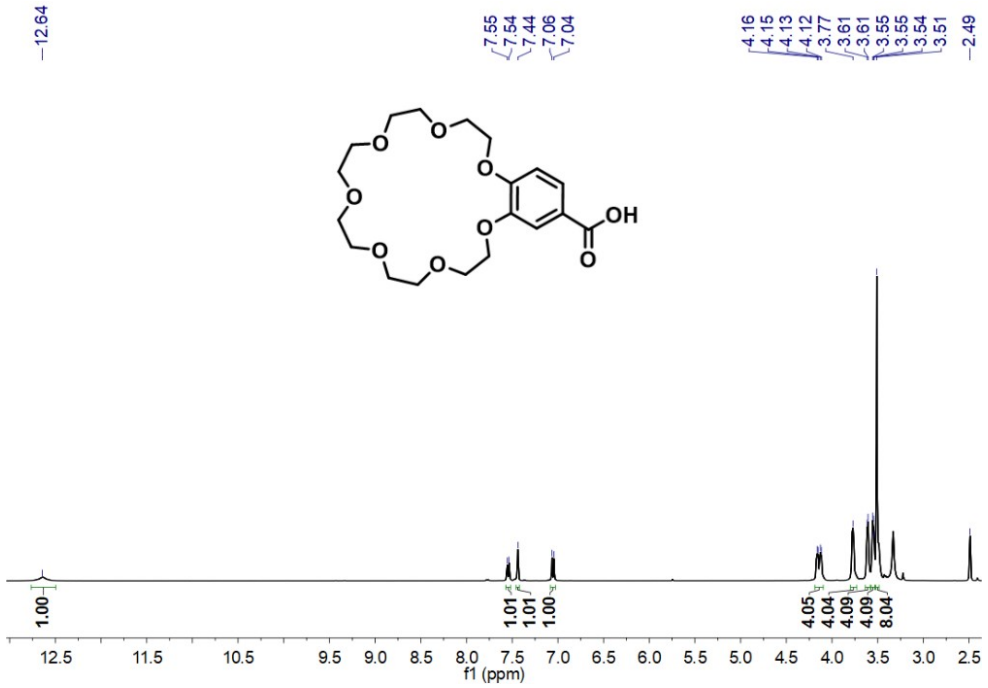

Fig. S2 ^{1}H NMR spectrum (400 MHz, DMSO-d_6, 298 K) of compound **H-2**.

Synthesis of compounds **H-3** and **H-4**

Under a nitrogen atmosphere, compound **H-2** (0.50 g, 1.25 mmol) was added to a reaction flask. Subsequently, DCM (6 mL) and DMF (0.30 mL) were added to dissolve the compound while stirring. Oxalyl chloride (0.48 g, 3.75 mmol) was then added under ice-bath conditions, followed by a three-hour reaction at room temperature to afford compound **H-3**. Then, 2-bromoethanol (1.55 g, 12.50 mmol) was added with continuous stirring, and the reaction was allowed to proceed for 4 hours at room temperature. After completion of the reaction, the solvent was removed under reduced pressure, and the crude product was purified by silica gel column chromatography (DCM/CH_3OH = 100:1, *v*/*v*) to afford compound **H-4** as a yellow oil (0.53 g, 1.05 mmol, yield: 83%). ^{1}H NMR (400 MHz, $CDCl_3$, 298 K) δ 7.68 (d, J = 8.4 Hz, 1H), 7.54 (s, 1H), 6.87 (d, J = 8.4 Hz, 1H), 4.58 (t, J = 6.1 Hz, 2H), 4.22 – 4.18 (m, 4H), 3.96 – 3.92 (m, 4H), 3.81 – 3.77 (m, 4H), 3.74 – 3.71 (m, 4H), 3.66 (s, 8H), 3.61 (t, J = 6.1 Hz, 2H). HR-ESI-MS m/z: [**H-4** + H]$^+$ calcd for $[C_{21}H_{32}O_9Br]^+$, 507.1225; found: 507.1191.

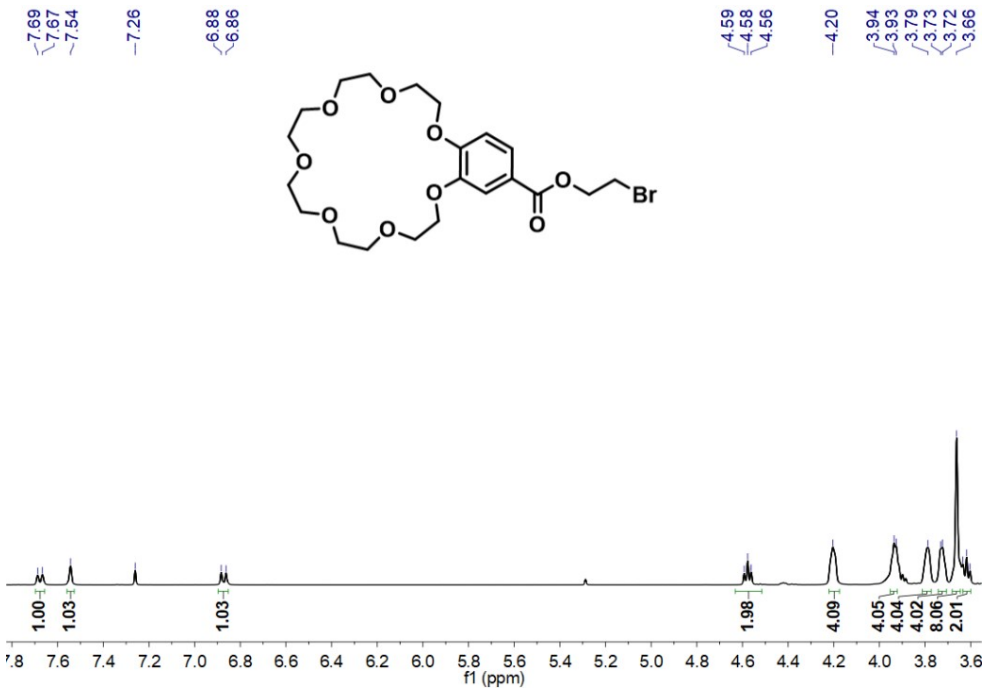

Fig. S3 ^{1}H NMR spectrum (400 MHz, $CDCl_3$, 298 K) of compound **H-4**.

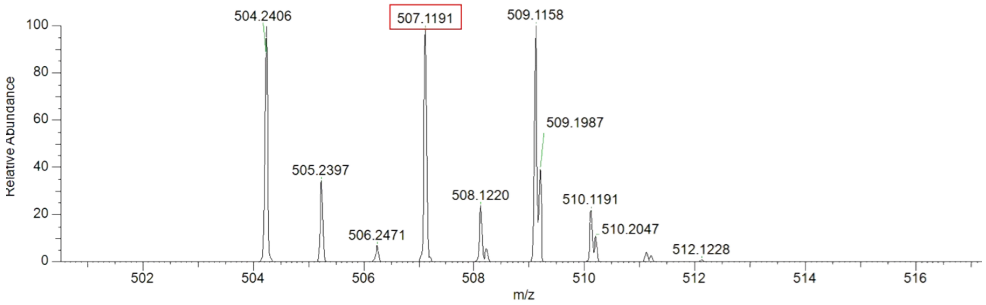

Fig. S4 HR-ESI-MS spectrum of compound **H-4**.

Synthesis of compound **H-5**

Under a nitrogen atmosphere, 4,4'-(2,2-bis(4-bromophenyl)ethene-1,1-diyl)diphenol (0.42 g, 0.80 mmol) and K_2CO_3 (2.87 g, 20.80 mmol) were added to a reaction flask. Subsequently, DMF (15 mL) was added, and the mixture was stirred until dissolution. Next, compound **H-4** (0.97 g, 1.92 mmol) dissolved in DMF (15 mL) was added to the reaction solution, and the mixture was refluxed overnight. After completion of the reaction, the solvent was removed under reduced pressure, and the crude product was purified by silica gel column chromatography (DCM/CH_3OH = 100:1, *v*/*v*) to afford compound **H-5** as a yellow oil (0.64 g, 0.46 mmol, yield: 58%). ^{1}H NMR (400 MHz, $CDCl_3$, 298 K) δ 7.67 (d, *J* = 10.1 Hz, 2H), 7.55 (s, 2H), 7.22 (d, *J* = 8.4 Hz, 4H), 6.90 (d, *J* = 8.6 Hz, 4H), 6.86 (dd, *J* = 8.4, 3.5 Hz, 6H), 6.68 (d, *J* = 8.7 Hz, 4H), 4.62 – 4.56 (m, 4H), 4.23 – 4.17(m, 12H), 3.95 – 3.91 (m, 8H), 3.82 – 3.78 (m, 8H), 3.75 – 3.71 (m, 8H), 3.66 (s, 16H). ^{13}C NMR (100 MHz, $CDCl_3$, 298 K) δ 166.27, 157.42, 153.11, 148.27, 142.69, 141.22, 136.88, 136.04, 133.10, 132.94, 132.67, 132.51, 131.12, 131.02, 124.22, 122.57, 120.41, 114.70, 114.05, 113.88, 112.28, 112.12,

71.37, 71.25, 71.1, 71.12, 71.05, 70.75, 70.58, 70.42, 69.87, 69.66, 69.51, 69.36, 69.11, 68.93, 65.93, 65.76, 63.16. HR-ESI-MS m/z: [**H-5** + H]$^+$ calcd for [$C_{68}H_{79}O_{20}Br_2$]$^+$, 1375.3506; found: 1375.3483.

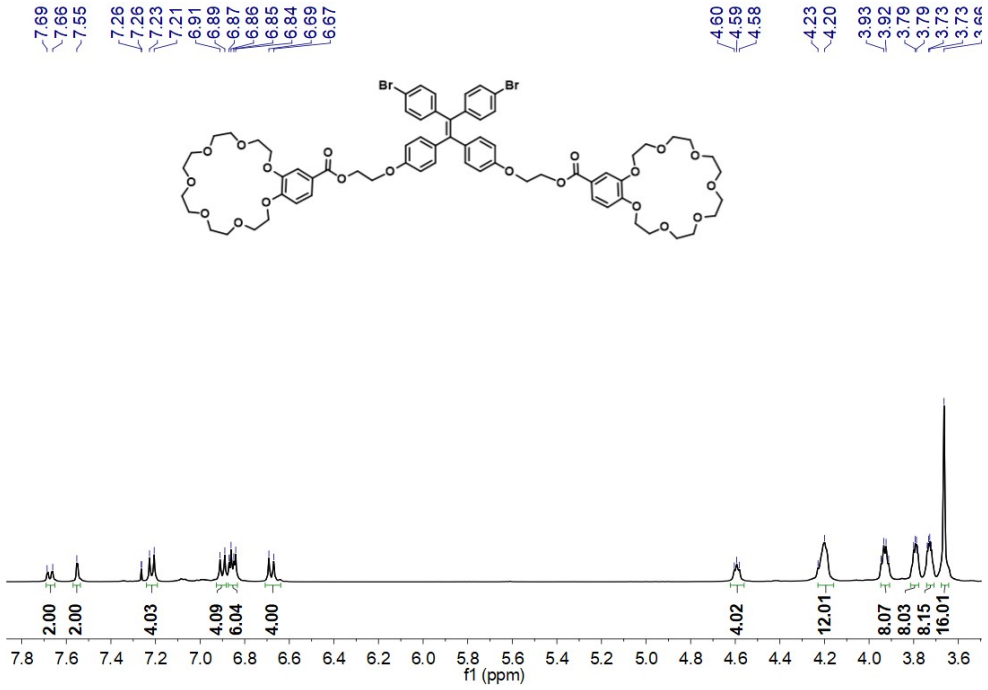

Fig. S5 ^{1}H NMR spectrum (400 MHz, $CDCl_3$, 298 K) of compound **H-5**.

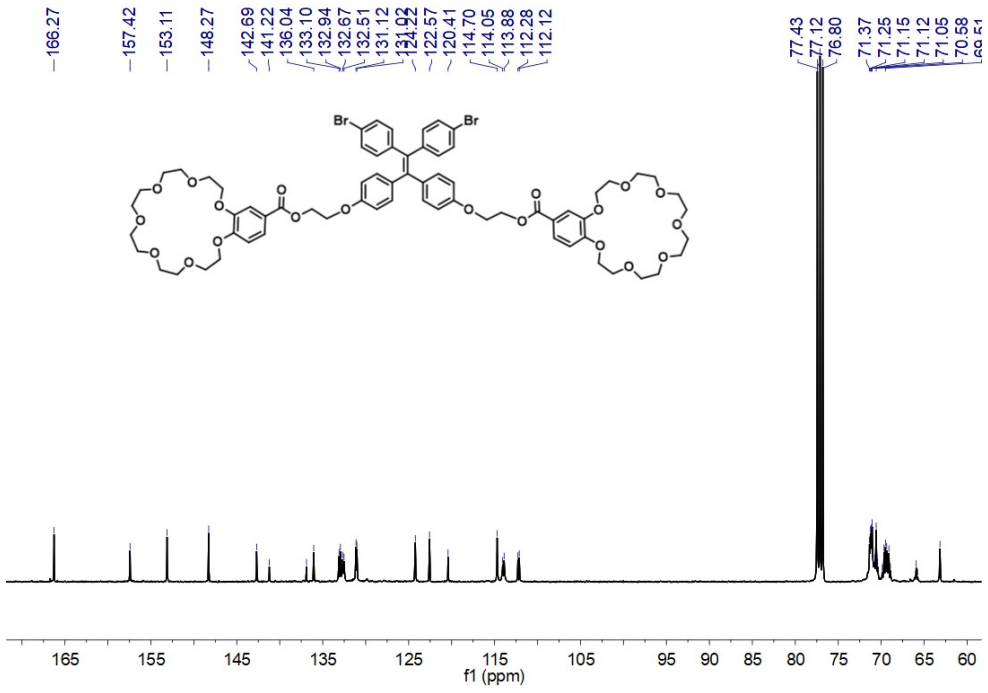

Fig. S6 ^{13}C NMR spectrum (100 MHz, $CDCl_3$, 298 K) of compound **H-5**.

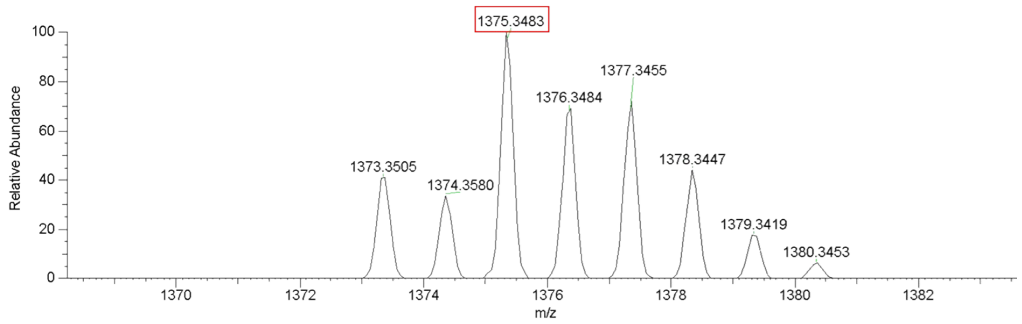

Fig. S7 HR-ESI-MS spectrum of compound **H-5**.

Synthesis of compound **PyCE**

Under a nitrogen atmosphere, compound **H-5** (0.33 g, 0.24 mmol), pyridine-3-boronic acid (0.17 g, 1.44 mmol), and TBAB (0.01 g, 0.02 mmol) were added to a reaction flask. Subsequently, toluene (7 mL) was added, and the mixture was stirred to ensure complete dissolution. Potassium carbonate (0.40 g, 2.88 mmol) dissolved in H_2O (1 mL) was then added to the reaction vial. After stirring for 10 min, $Pd(PPh_3)_4$ (0.03 g, 0.03 mmol) was introduced into the reaction solution, and the reaction was heated to 80°C and stirred overnight. After completion of the reaction, the solvent was removed under reduced pressure, and the crude product was purified by silica gel column chromatography (DCM/CH_3OH = 100:1, *v*/*v*) to afford compound **PyCE** as a yellow powder (0.19 g, 0.14 mmol, yield: 58%). ^{1}H NMR (400 MHz, $CDCl_3$, 298 K) δ 8.82 (s, 2H), 8.55 (d, *J* = 4.6 Hz, 2H), 7.87 (d, *J* = 7.9 Hz, 2H), 7.67 (d, *J* = 8.4 Hz, 2H), 7.55 (s, 2H), 7.39 –7.31 (m, 6H), 7.16 (d, *J* = 8.1 Hz, 4H), 7.00 (d, *J* = 8.5 Hz, 4H), 6.86 (d, *J* = 8.5 Hz, 2H), 6.71 (d, *J* = 8.6 Hz, 4H), 4.65 – 4.53 (m, 4H), 4.26 – 4.16 (m, 12H), 3.96 – 3.91 (m, 8H), 3.83 – 3.77 (m, 8H), 3.76 – 3.71 (m, 8H), 3.67 (s, 16H). ^{13}C NMR (100 MHz, $CDCl_3$, 298 K) δ 165.25, 156.39, 152.07, 147.23, 146.57, 146.36, 146.27, 143.17, 140.27, 136.74, 135.39, 134.01, 133.70, 131.73, 131.59, 131.22, 131.11, 125.41, 123.13, 122.75, 121.50, 113.68, 112.98, 112.81, 111.24, 111.07, 70.30, 70.22, 70.08, 69.98, 69.52, 68.59, 68.44, 68.32, 68.06, 64.86, 62.07. HR-ESI-MS m/z: [**PyCE** + H]$^+$ calcd for $[C_{78}H_{87}O_{20}N_2]^+$, 1371.5847; found: 1371.5814. DOSY NMR (400 MHz, $CDCl_3$, 298 K) spectrum was recorded for **PyCE**, revealing a diffusion coefficient (*D*) of 3.55 × 10^{-6} cm^2/sec.

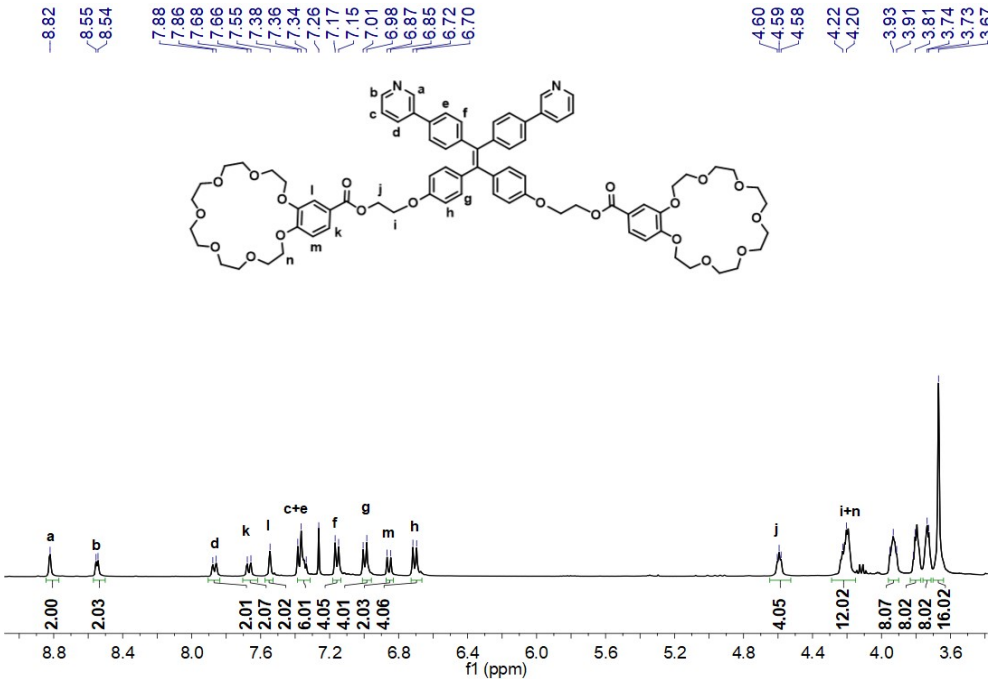

Fig. S8 ^{1}H NMR spectrum (400 MHz, $CDCl_3$, 298 K) of compound **PyCE**.

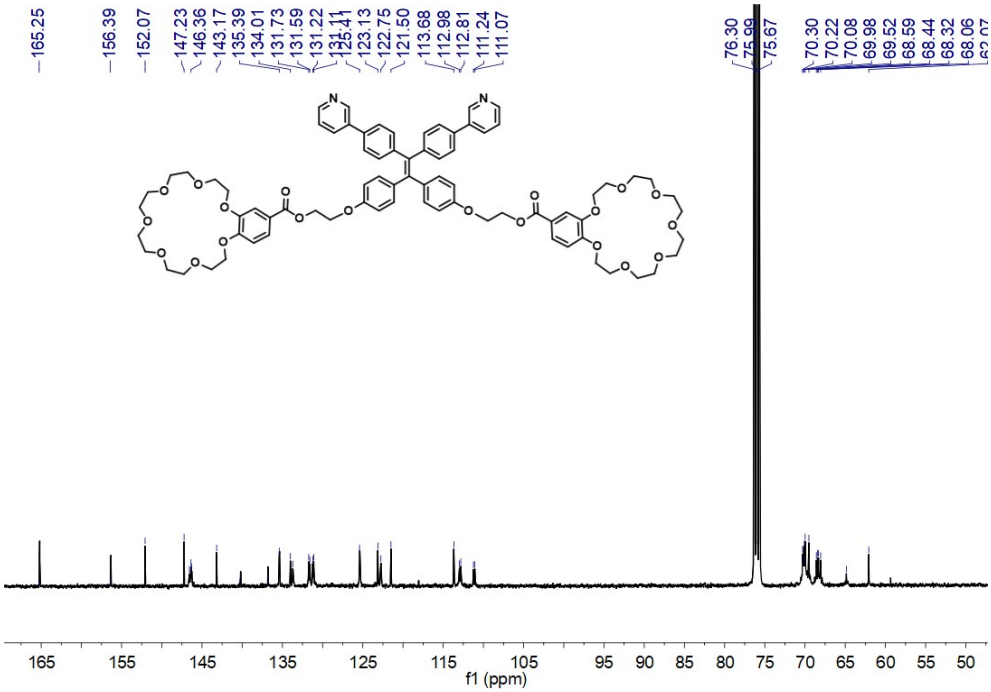

Fig. S9 ^{13}C NMR spectrum (100 MHz, $CDCl_3$, 298 K) of compound **PyCE**.

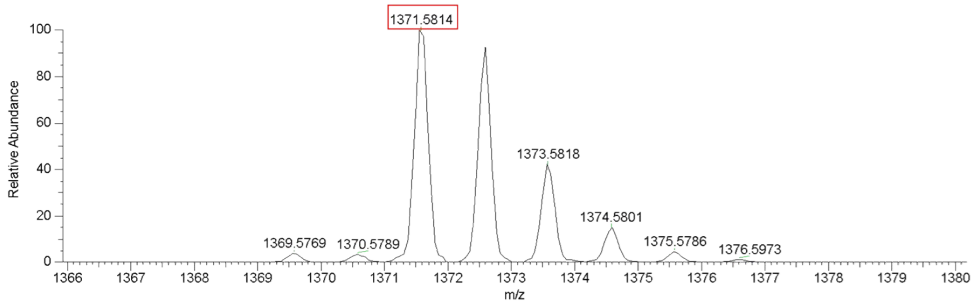

Fig. S10 HR-ESI-MS spectrum of compound **PyCE**.

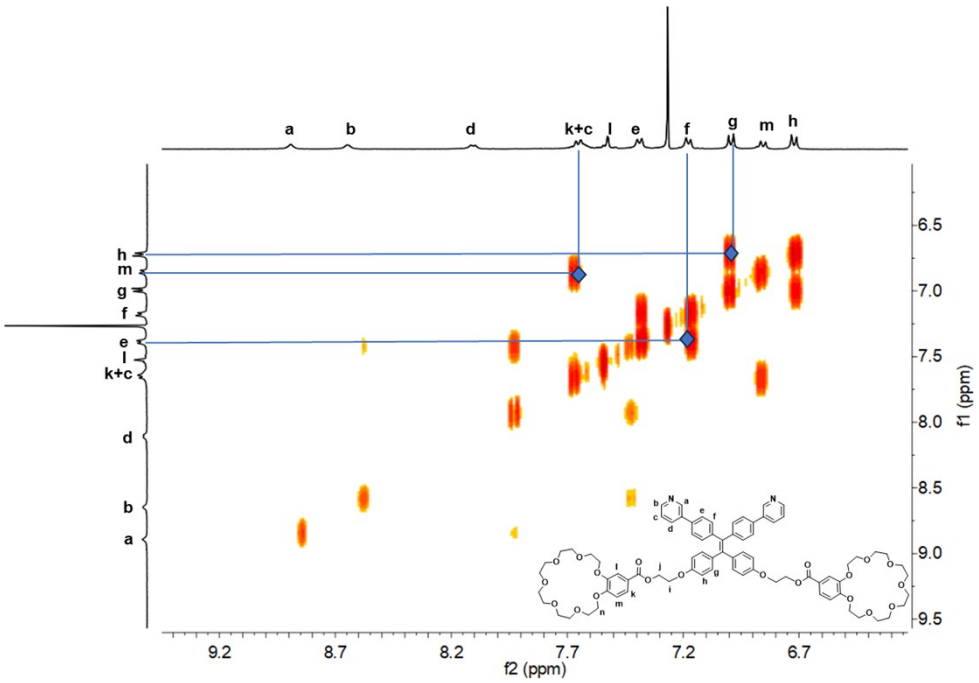

Fig. S11 ^{1}H-^{1}H COSY NMR spectrum (400 MHz, $CDCl_3$, 298 K) of compound **PyCE**.

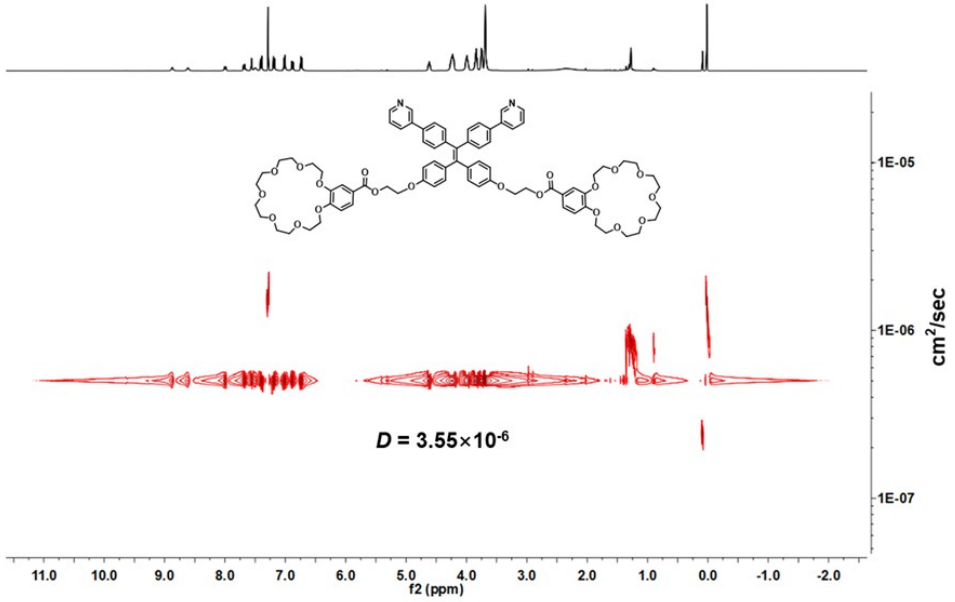

Fig. S12 DOSY NMR spectrum (400 MHz, $CDCl_3$, 298 K) of compound **PyCE**.

Synthesis of model ligand Py

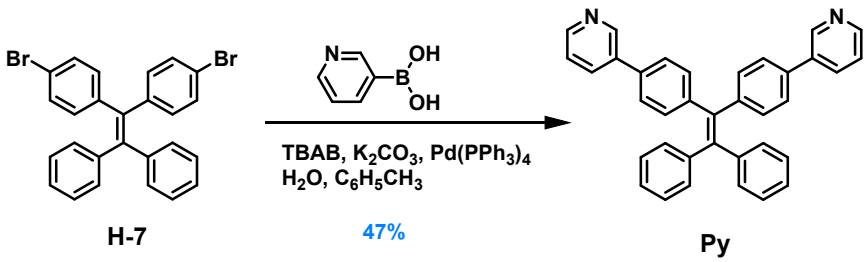

Scheme S2 Synthesis route of model ligand **Py**.

Synthesis of compound **Py**[5]

Under a nitrogen atmosphere, compound **H-7** (0.40 g, 0.82 mmol), pyridine-3-boronic acid (0.51 g, 4.12 mmol), and TBAB (0.03 g, 0.08 mmol) were added to a reaction flask. Subsequently, toluene (10 mL) was added, and the mixture was stirred to ensure complete dissolution. Potassium carbonate (1.36 g, 9.83 mmol) dissolved in H_2O (1 mL) was then added to the reaction vial. After stirring for 10 min, $Pd(PPh_3)_4$ (0.10 g, 0.08 mmol) was introduced into the reaction solution, and the reaction was heated to 80°C and stirred overnight. After completion of the reaction, the solvent was removed under reduced pressure, and the crude product was purified by silica gel column chromatography (DCM/CH_3OH = 100:1, *v*/*v*) to afford compound **Py** as a white powder (0.19 g, 0.39 mmol, yield: 47%). ^1H NMR (400 MHz, $CDCl_3$, 298 K) δ 8.82 (d, *J* = 1.9 Hz, 2H), 8.56 (dd, *J* = 4.8, 1.3 Hz, 2H), 7.91 – 7.85 (m, 2H), 7.37 (d, *J* = 8.3 Hz, 6H), 7.21 – 7.11 (m, 10H), 7.08 (dd, *J* = 6.7, 3.0 Hz, 4H). DOSY NMR (400 MHz, $CDCl_3$, 298 K) spectrum was recorded for **Py**, revealing a diffusion coefficient (*D*) of 6.13 × 10^{-6} cm^2/sec.

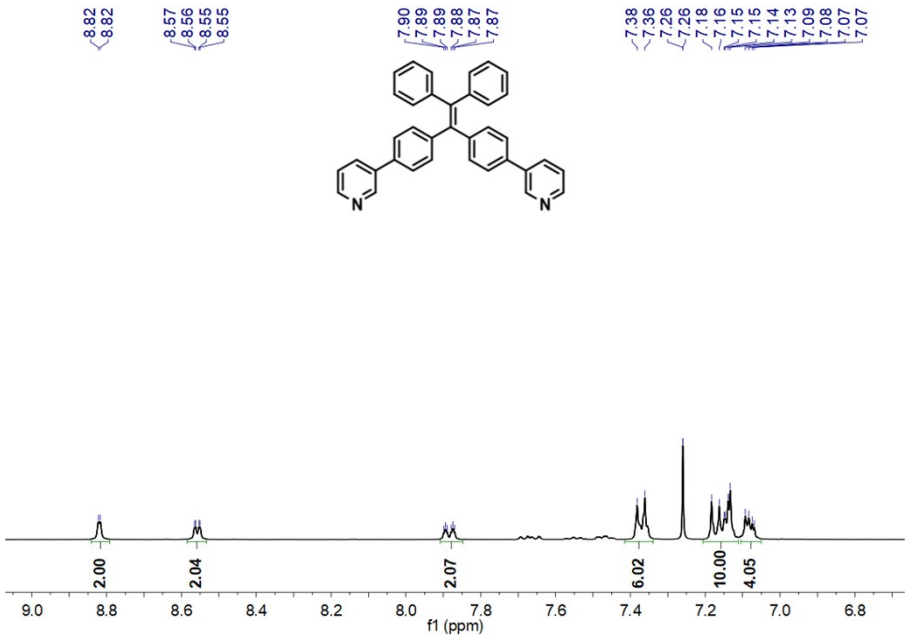

Fig. S13 ^1H NMR spectrum (400 MHz, $CDCl_3$, 298 K) of compound **Py**.

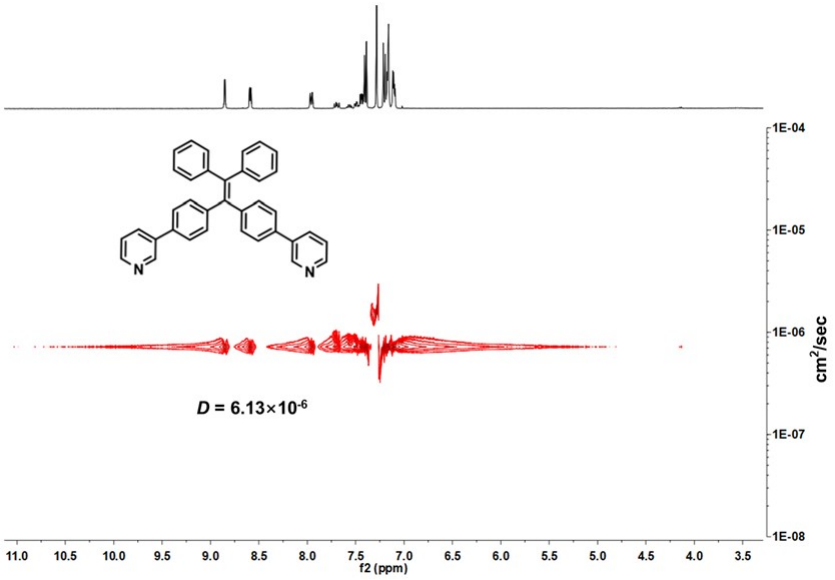

Fig. S14 DOSY NMR spectrum (400 MHz, $CDCl_3$, 298 K) of compound **Py**.

Synthesis of guest molecule G

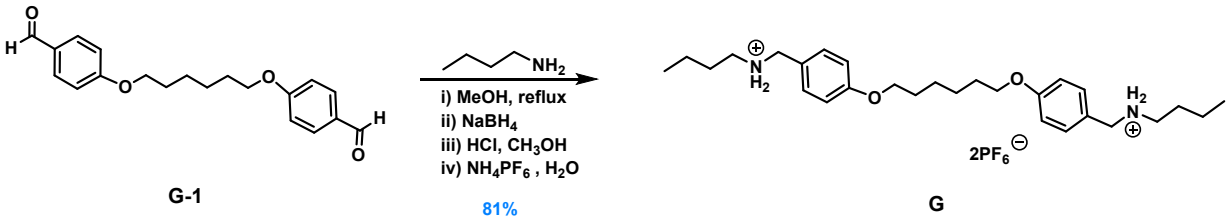

Scheme S3 Synthesis route of guest molecule **G**.

Synthesis of compound **G**[6]

Under a nitrogen atmosphere, compound **G-1** (0.40 g, 1.21 mmol) and *n*-butylamine (0.19 g, 2.66 mmol) were sequentially heated to reflux overnight in CH_3OH (12 mL). After cooling the reaction mixture to room temperature, $NaBH_4$ (0.18 g, 4.84 mmol) was added to the stirred solution in batches over a period of 1 hour under ice-bath conditions. The solution was stirred under ambient conditions for another 24 hours, after which 3 M HCl was added to neutralize the excess $NaBH_4$. The mixture was filtered and CH_3OH was removed by rotary evaporator. H_2O was added and the solution was added to saturated NH_4PF_6 solution to produce a precipitate, which was collected by filtration and recrystallized three times in deionized H_2O to afford compound **G** as a white powder (0.72 g, 0.98 mmol, yield: 81%). ^{1}H NMR (400 MHz, CD_3CN, 298 K) δ 7.36 (d, J = 8.1 Hz, 4H), 6.96 (d, J = 8.0 Hz, 4H), 6.66 (brs, 4H), 4.08 (s, 4H), 4.01 (t, J = 6.5 Hz, 4H), 3.03 – 2.95 (m, 4H), 1.79 (d, J = 6.2 Hz, 4H), 1.65 – 1.58 (m, 4H), 1.52 (s, 4H), 1.39 – 1.32 (m, 4H), 0.93 (t, J = 7.3 Hz, 6H).

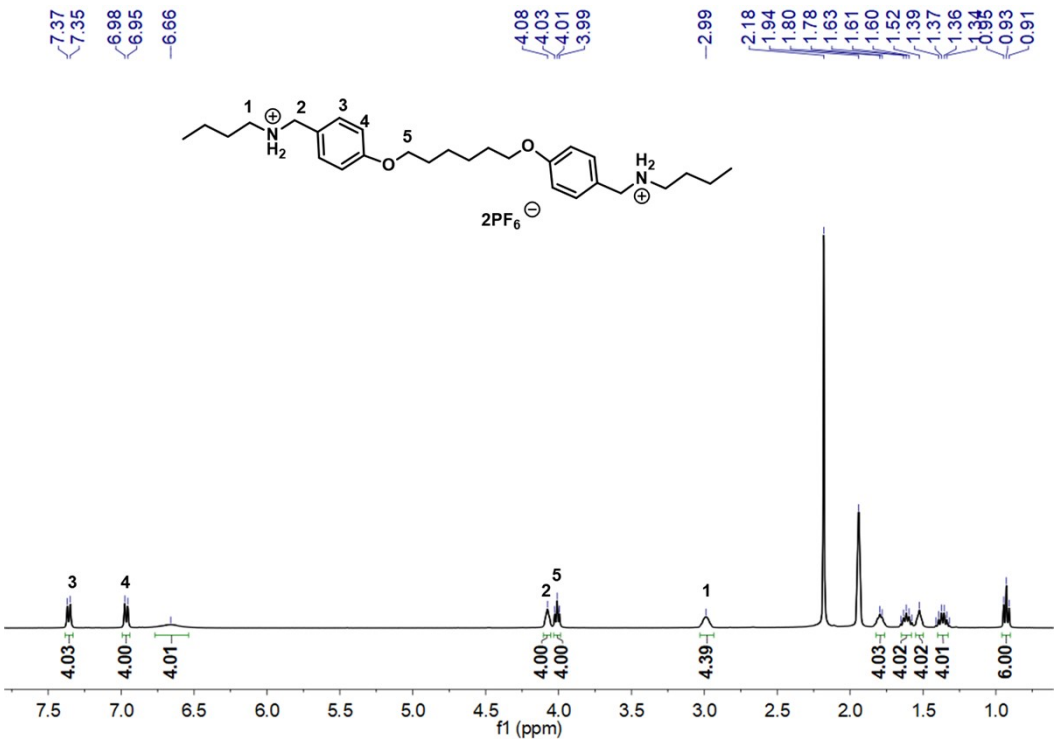

Fig. S15 ^{1}H NMR spectrum (400 MHz, CD_3CN, 298 K) of compound **G**.

Synthesis of platinum metal acceptor M[7]

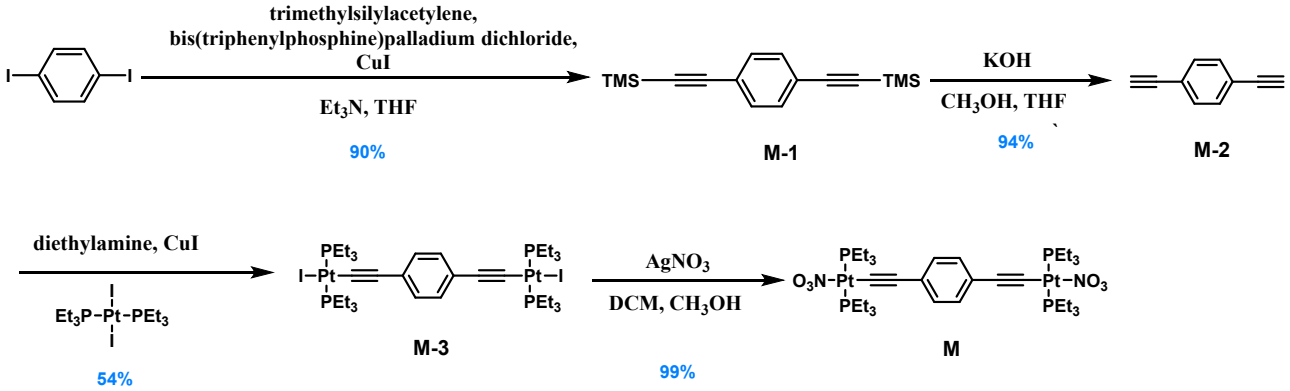

Scheme S4 Synthesis route of platinum metal acceptor **M**.

Synthesis of compound **M-1**

Under a nitrogen atmosphere, bis(triphenylphosphine)palladium dichloride (0.21 g, 0.30 mmol), 1,4-diiodobenzene (1 g, 3.03 mmol), trimethylsilylacetylene (0.74 g, 7.58 mmol), triethylamine (2 mL), and THF (12 mL) were added to the reaction flask. After stirring at room temperature for 10 minutes, CuI (0.03 g, 0.15 mmol) was added. The reaction mixture was then heated to 60°C and reacted in the dark for 24 hours. After completion of the reaction, the solvent was removed under reduced pressure, and the crude product was purified by silica gel column chromatography (PE) to afford compound **M-1** as a white powder (0.74 g, 2.73 mmol, yield: 90%). ^{1}H NMR (400 MHz, $CDCl_3$, 298 K) δ 7.39 (s, 4H), 0.24 (s, 18H).

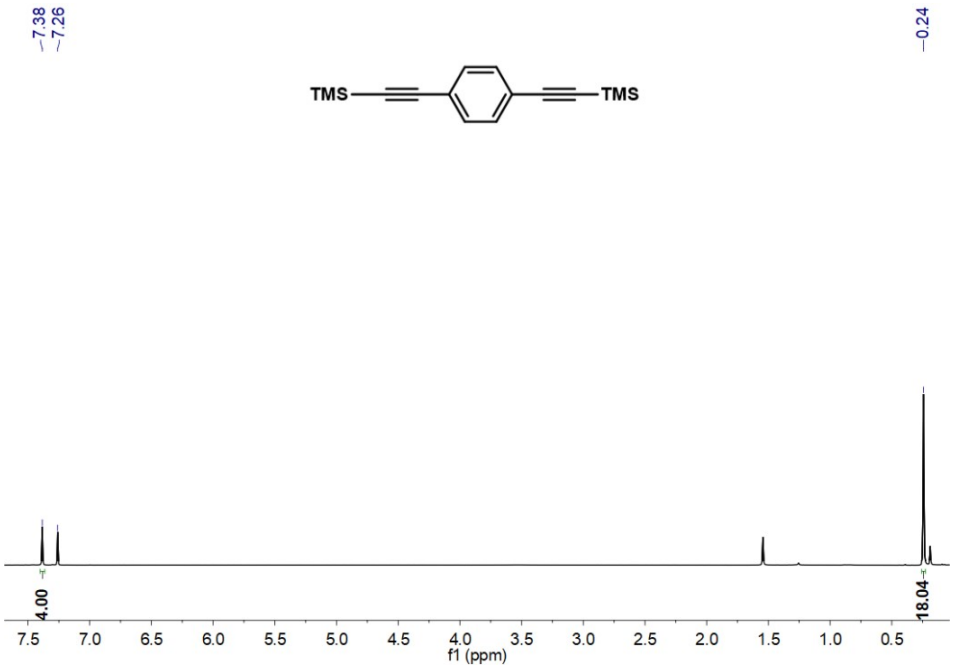

Fig. S16 ^{1}H NMR spectrum (400 MHz, $CDCl_3$, 298 K) of compound **M-1**.

Synthesis of compound **M-2**

Compound **M-1** (0.73 g, 1.98 mmol) was dissolved in mixture of CH_3OH/THF (36 mL, *v*/*v* = 1:1), and KOH aqueous solution (1 M, 5.95 mL) was added to the reaction flask and stirred at room temperature for 5 hours. After completion of the reaction, the solvent was removed under reduced pressure, and the crude product was purified by silica gel column chromatography (*n*-hexane/DCM = 4:1, *v*/*v*) to afford compound **M-2** as a white powder (0.24 g, 1.87 mmol, yield: 94%). ^{1}H NMR (400 MHz, $CDCl_3$, 298 K) δ 7.44 (s, 4H), 3.17 (s, 2H).

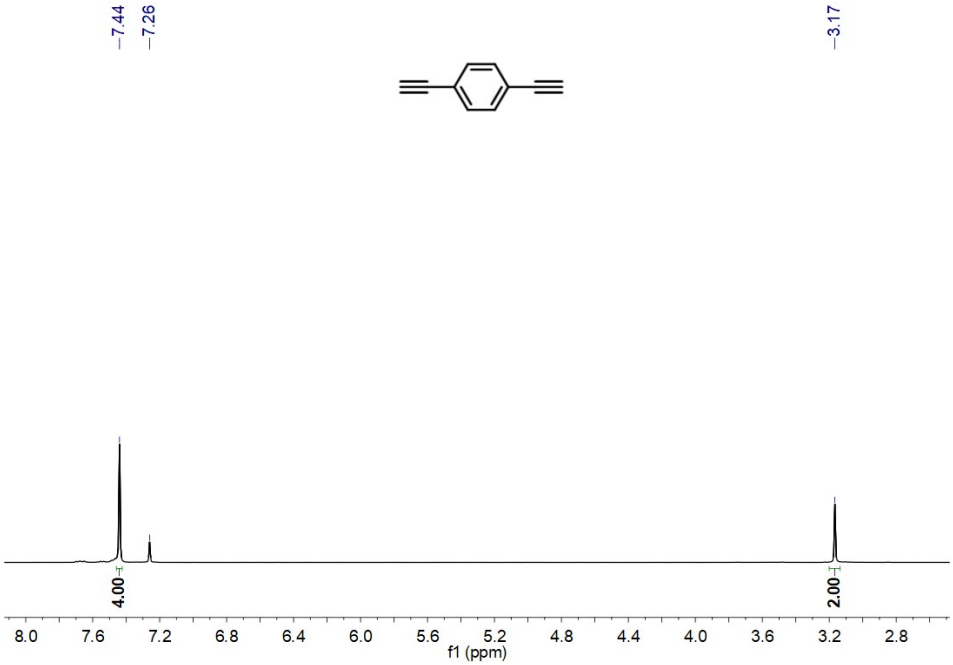

Fig. S17 ^{1}H NMR spectrum (400 MHz, $CDCl_3$, 298 K) of compound **M-2**.

Synthesis of compound **M-3**

Under a nitrogen atmosphere, compound **M-2** (0.05 g, 0.41 mmol) and $Pt(PEt_3)_2I_2$ (0.70 g, 1.02 mmol) were added to the reaction flask, followed by the addition of toluene (10 mL) and triethylamine (5 mL). After stirring for 10 minutes, CuI (0.01 g, 0.05 mmol) was added and the reaction was allowed to proceed at room temperature in the dark for 24 hours. After completion of the reaction, the solvent was removed under reduced pressure, and the crude product was purified by silica gel column chromatography (*n*-hexane/DCM = 4:1, *v*/*v*) to afford compound **M-3** as a white powder (0.28 g, 0.22 mmol, yield: 54%). ^{1}H NMR (400 MHz, $CDCl_3$, 298 K) δ 7.14 (s, 4H), 2.26 – 2.17 (m, 24H), 1.23 – 1.10 (m, 36H). ^{31}P NMR (162 MHz, $CDCl_3$, 298 K) δ (ppm): 8.43 ppm (s, ^{195}Pt satellites, $^1J_{Pt-P}$ = 2321 Hz).

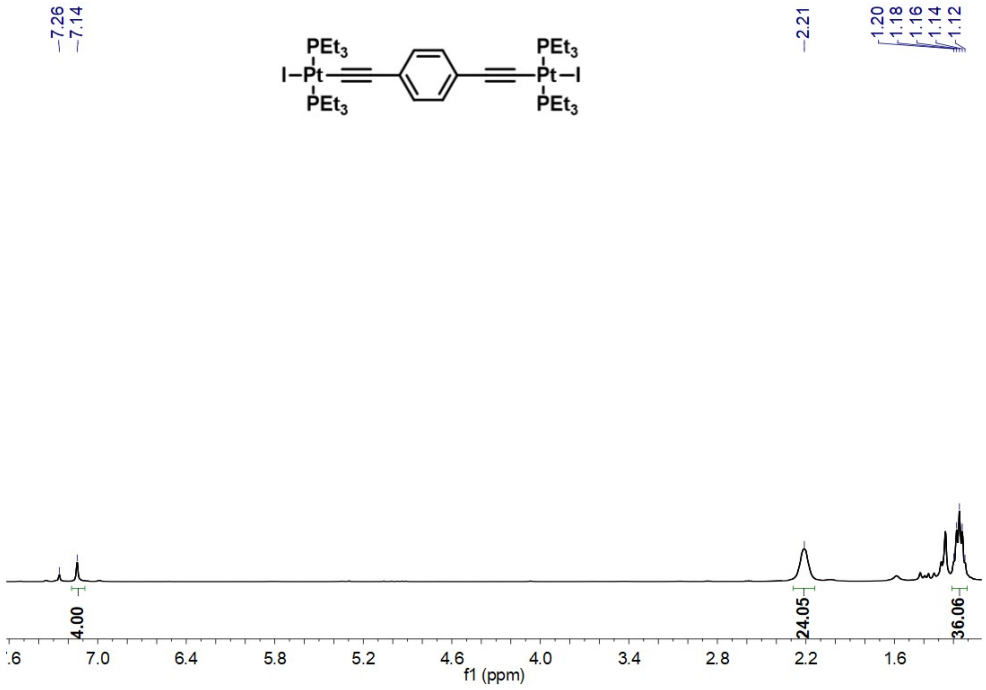

Fig. S18 ^{1}H NMR spectrum (400 MHz, $CDCl_3$, 298 K) of compound **M-3**.

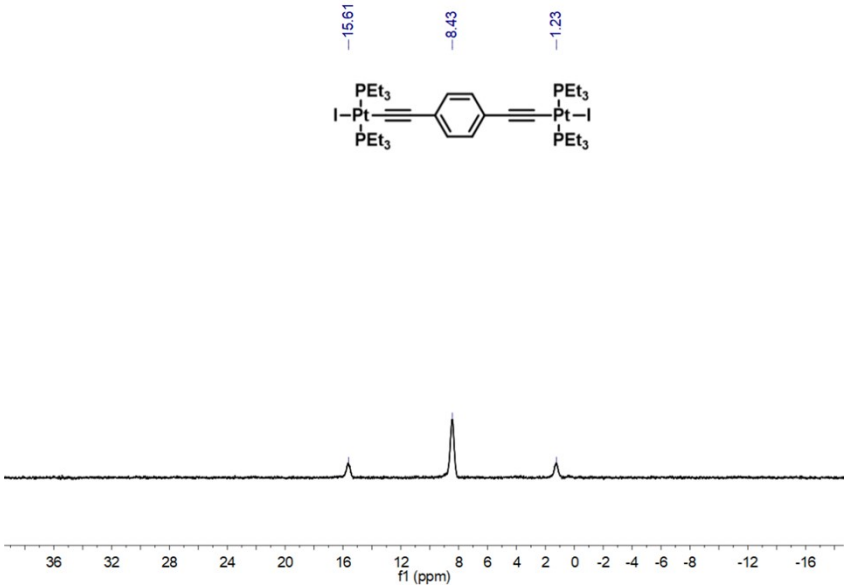

Fig. S19 ^{31}P NMR spectrum (162 MHz, $CDCl_3$, 298 K) of compound **M-3**.

Synthesis of compound **M**

Under a nitrogen atmosphere, compound **M-3** (0.15 g, 0.12 mmol) and $AgNO_3$ were added to the reaction flask. The mixture of dry DCM/CH_3OH (5 mL, *v/v* = 1:1) was added, and the reaction was stirred in the dark for 4 hours. The resulting precipitate was removed by filtration, and the filtrate was concentrated under a stream of nitrogen, followed by further drying under vacuum at room temperature to afford compound **M** (0.13 g, 0.12 mmol, yield: 99%). ^{1}H NMR (400 MHz, $CDCl_3$, 298 K) δ 7.15 (s, 4H), 1.98 – 1.90 (m, 24H), 1.32 – 1.10 (m, 48H). ^{31}P NMR (162 MHz, $CDCl_3$, 298 K) δ (ppm): 20.01 ppm (s, ^{195}Pt satellites, $^1J_{Pt-P}$ = 2430 Hz).

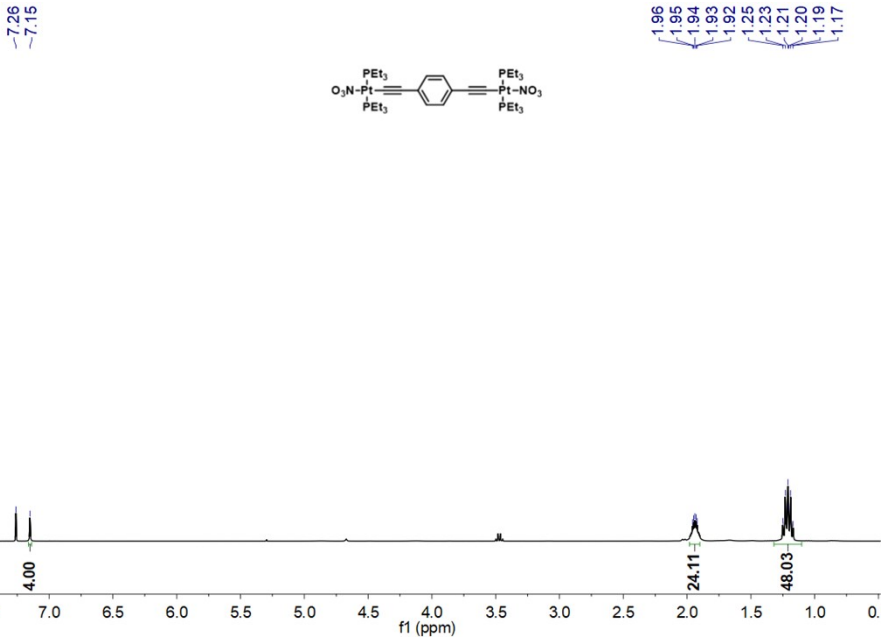

Fig. S20 ^{1}H NMR spectrum (400 MHz, $CDCl_3$, 298 K) of compound **M**.

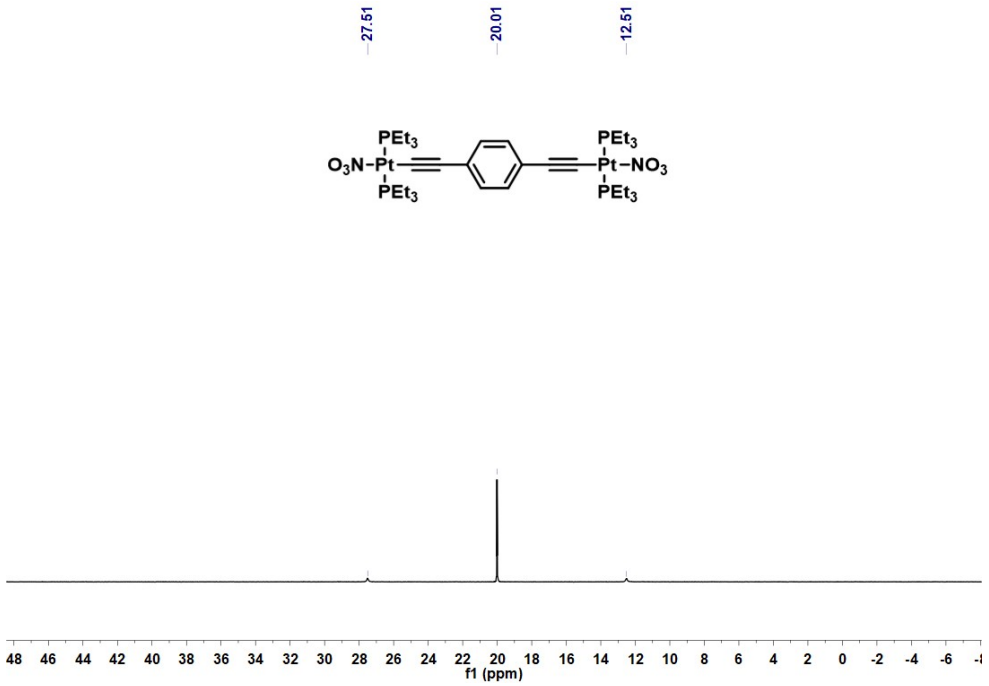

Fig. S21 ^{31}P NMR spectrum (162 MHz, $CDCl_3$, 298 K) of compound **M**.

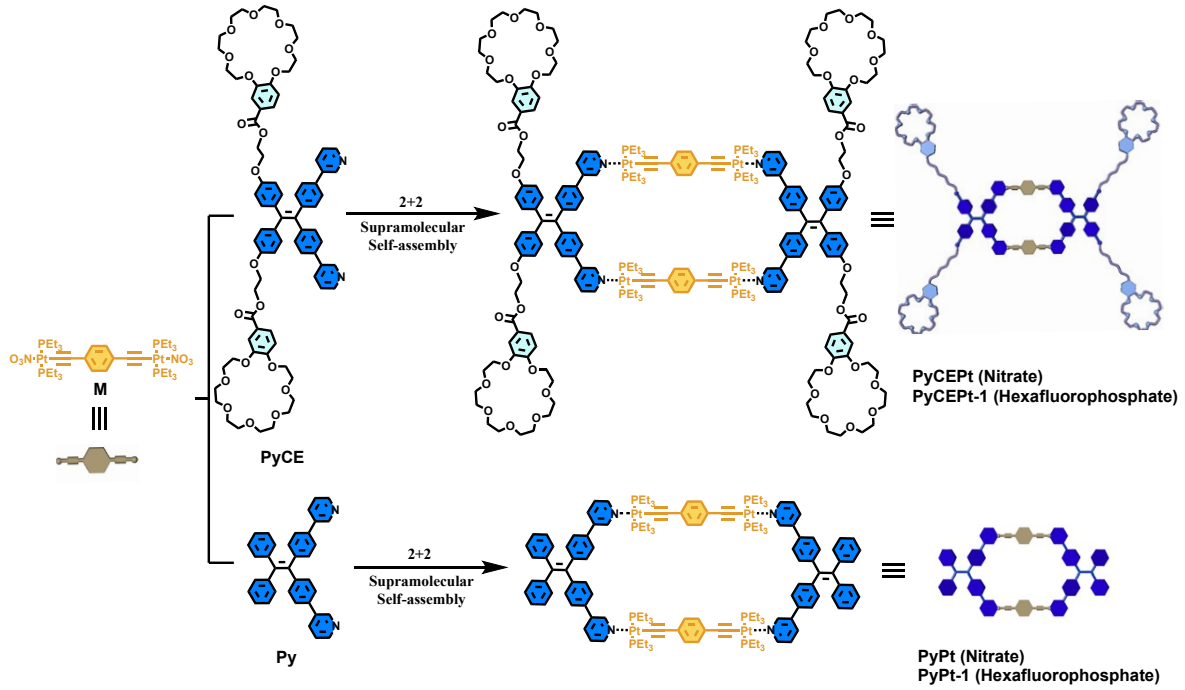

Fig. S22 Schematic illustration of the design of metallacycles **PyCEPt** and **PyPt** synthesized through coordination-driven self-assembly.

Synthesis of metallacycle PyCEPt

Compound **PyCE** (13.70 mg, 0.01 mmol) and **M** (11.10 mg, 0.01 mmol) were weighed separately and dissolved in dry DCM (1 mL). The self-assembly was done by slowly adding compound **M** to the solution of compound **PyCE**, and the whole reaction mixture was stirred for 24 hours at room temperature. The solvent was evaporated under nitrogen flow, and the self-assembled

metallacycle was isolated and recrystallized with DCM-ethyl ether. The precipitated residue was redissolved in dry DCM (2.0 mL) and filtered through glass wool. The solvent was removed by nitrogen flow, and the compound was further dried under vacuum at room temperature to yield compound **PyCEPt** as a brown powder (37.40 mg, 0.01 mmol, yield: 78%). ^{1}H NMR (400 MHz, $CDCl_3$, 298 K) δ 9.03 (s, 4H), 8.73 (d, J = 4.5 Hz, 4H), 8.12 (d, J = 10.3 Hz, 4H), 7.96 – 7.87 (m, 4H), 7.71 (d, J = 8.9 Hz, 4H), 7.57 (s, 4H), 7.51 (s, 8H), 7.31 (d, J = 7.6 Hz, 8H), 7.11 (dd, J = 15.8, 8.1 Hz, 16H), 6.91 (d, J = 8.6 Hz, 4H), 6.77 (d, J = 8.6 Hz, 8H), 4.67 – 4.60 (m, 8H), 4.25 – 4.19 (m, 24H), 3.95 – 3.90 (m, 16H), 3.79 – 3.75 (m, 16H), 3.70 – 3.73 (m, 16H), 3.67 – 3.64 (m, 32H), 1.82 – 1.72 (m, 48H), 1.19 – 1.11 (m, 72H). ^{31}P NMR (162 MHz, $CDCl_3$, 298 K) δ 12.52 (s, ^{195}Pt satellites, $^{1}J_{Pt\text{-}P}$ = 2253 Hz). DOSY NMR (400 MHz, $CDCl_3$, 298 K) spectrum was recorded for **PyCEPt**, revealing a diffusion coefficient (D) of 1.56 × 10^{-6} cm^2/sec.

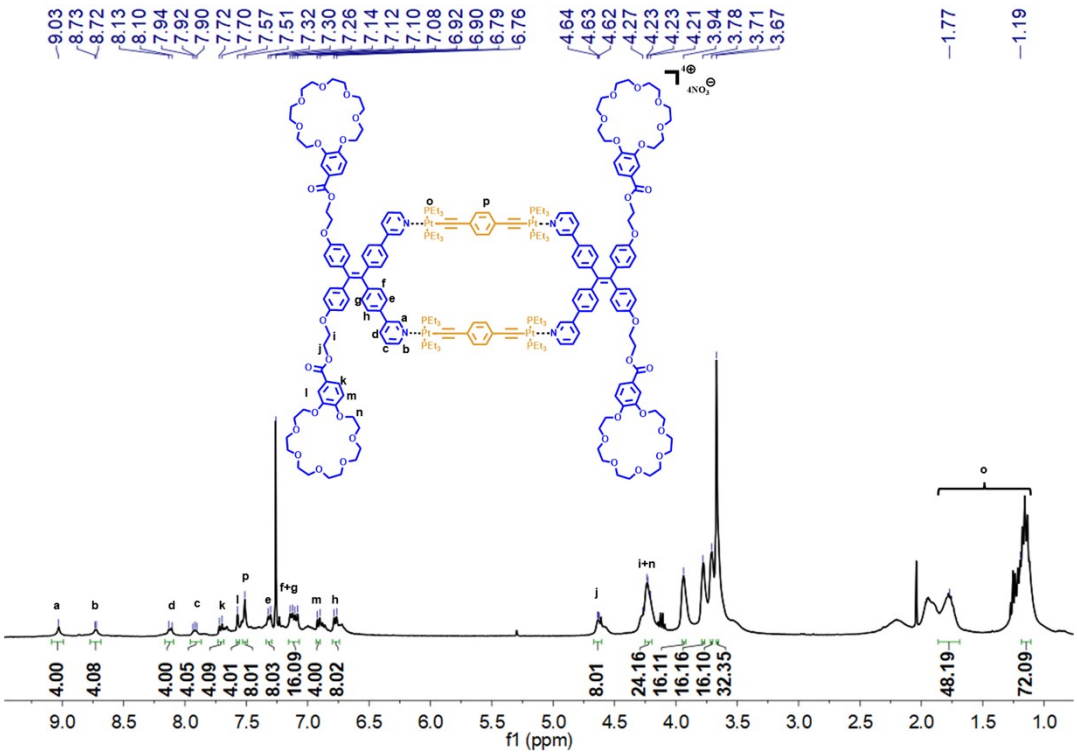

Fig. S23 ^{1}H NMR spectrum (400 MHz, $CDCl_3$, 298 K) of compound **PyCEPt**.

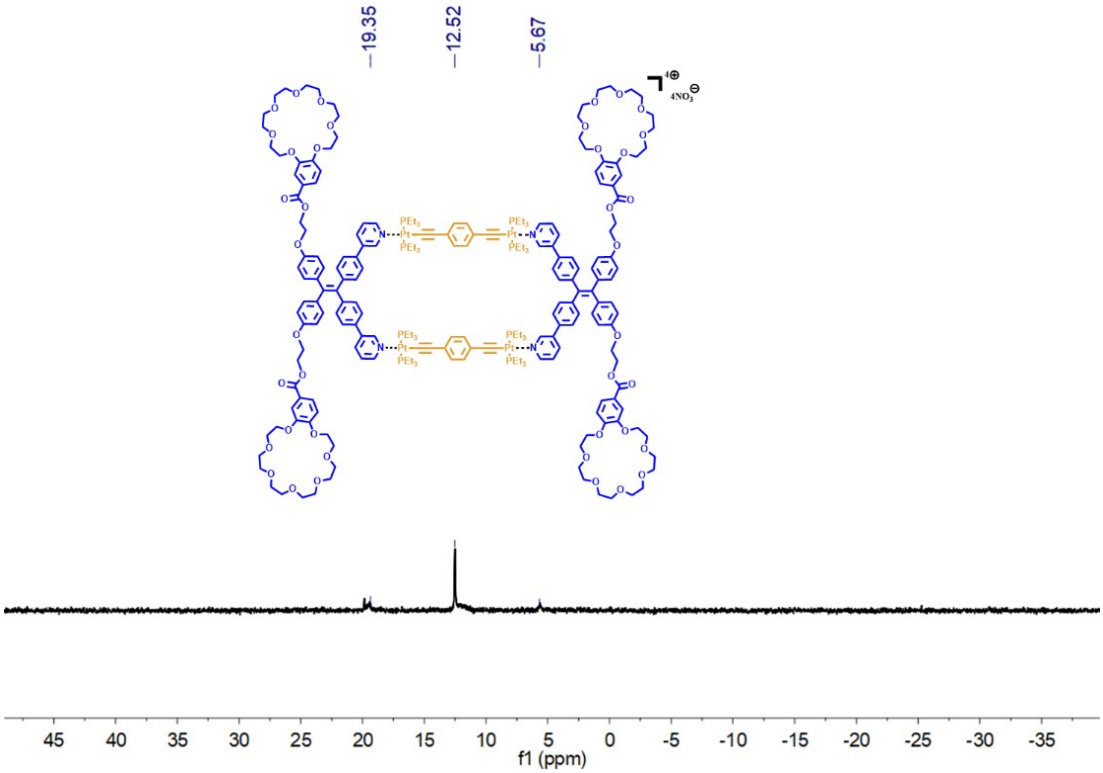

Fig. S24 ^{31}P NMR spectrum (162 MHz, $CDCl_3$, 298 K) of compound **PyCEPt**.

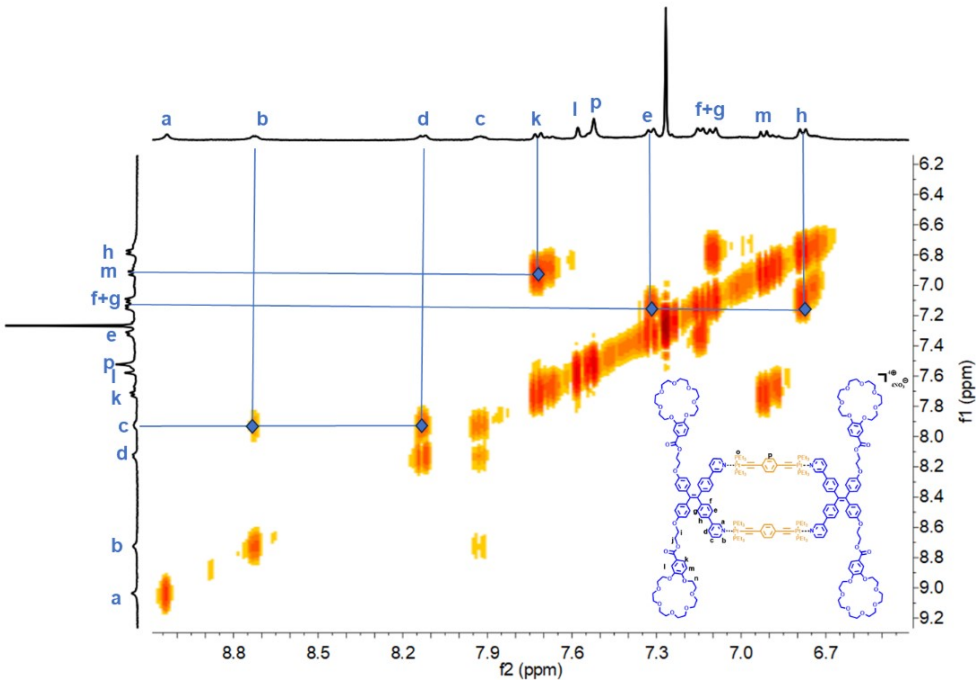

Fig. S25 ^{1}H-^{1}H COSY NMR spectrum (400 MHz, $CDCl_3$, 298 K) of compound **PyCEPt**.

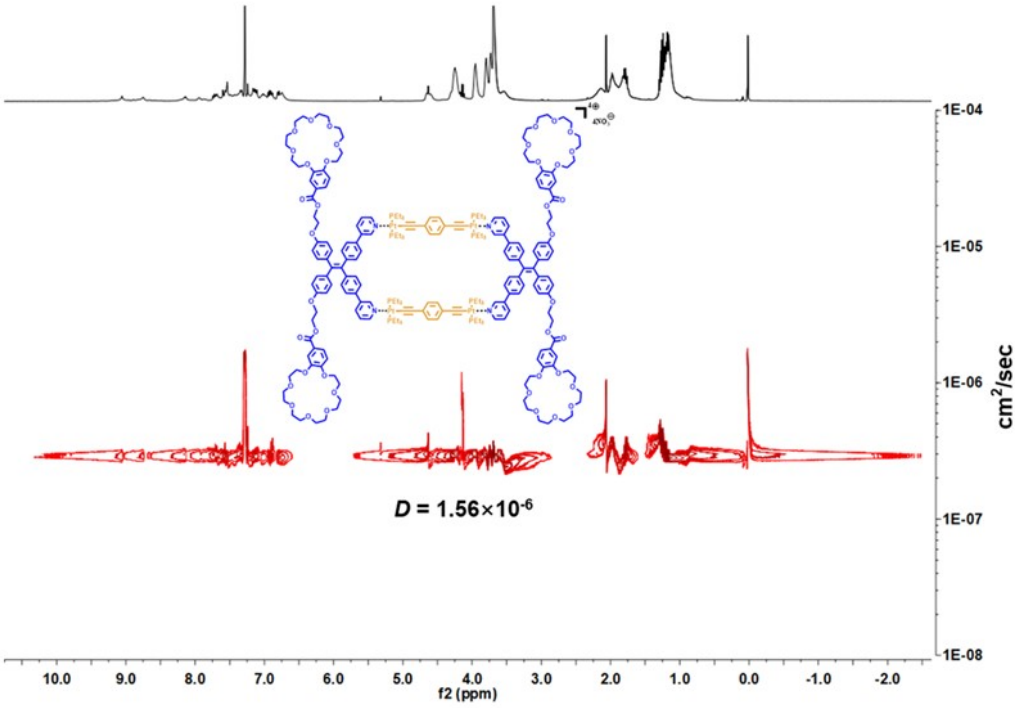

Fig. S26 DOSY NMR spectrum (400 MHz, $CDCl_3$, 298 K) of compound **PyCEPt**.

Compound **PyCEPt** (18.70 mg, 0.01 mmol) was dissolved in 1 mL of DMF in a 10 mL vial, followed by the addition of a saturated aqueous solution of KPF_6 (2 mL) to precipitate the product. The reaction mixture was centrifuged; the resulting solid was washed repeatedly with deionized water and vacuum-dried at room temperature, yielding the yellow precipitate **PyCEPt-1**. ^{1}H NMR (400 MHz, acetone-d_6, 298 K) δ 9.18 (s, 4H), 9.08 (d, J = 0.6 Hz, 4H), 8.95 (d, J = 5.5 Hz, 4H), 8.42 (d, J = 7.7 Hz, 4H), 8.35 (d, J = 8.5 Hz, 4H), 7.91 – 7.86 (m, 4H), 7.65 (dd, J = 17.6, 7.4 Hz, 8H), 7.59 – 7.53 (m, 8H), 7.33 – 7.20 (m, 16H), 7.09 (d, J = 8.5 Hz, 4H), 7.03 (d, J = 8.5 Hz, 8H), 6.84 (d, J = 8.7 Hz, 8H), 4.63 – 4.58 (m, 8H), 4.38 – 4.30 (m, 8H), 4.27 – 4.17 (m, 16H), 3.91 – 3.85 (m, 16H), 3.73 – 3.69 (m, 16H), 3.68 – 3.62 (m, 16H), 3.62 – 3.56 (m, 32H), 1.97 – 1.89 (m, 48H), 1.41 – 1.06 (m, 72H). ^{13}C NMR (100 MHz, acetone-d_6, 298 K) δ 166.47, 153.63, 150.89, 149.03, 133.51, 131.74, 127.99, 124.84, 123.75, 114.96, 114.56, 112.94, 70.82, 70.63, 70.58, 70.37, 70.10, 69.97, 68.97, 68.83, 66.96, 64.05, 15.17, 15.00, 14.83, 8.31. ^{31}P NMR (162 MHz, acetone-d_6, 298 K) δ 15.72 (s, ^{195}Pt satellites, $^1J_{Pt\text{-}P}$ = 2334 Hz). ESI-TOF-MS: calculated for [(**PyCEPt-1**)−4PF_6^-]$^{4+}$, 1178.9506; found, 1178.9152.

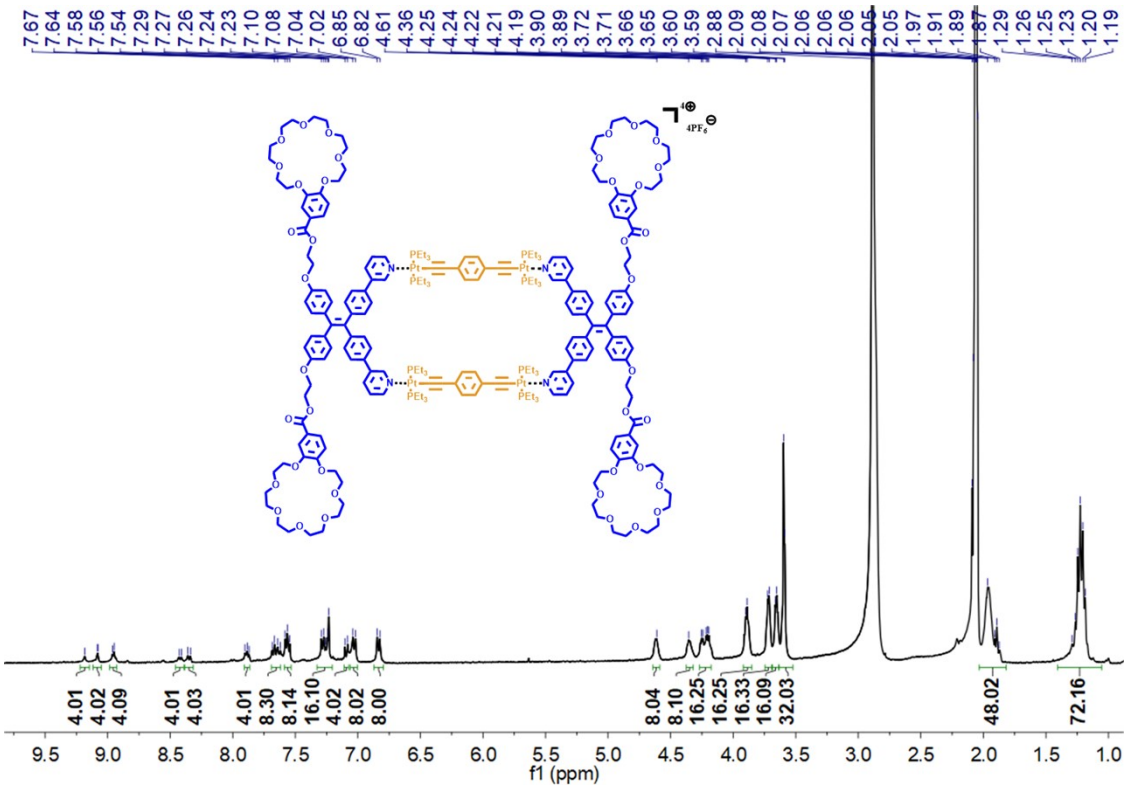

Fig. S27 ^{1}H NMR spectrum (400 MHz, acetone-d_6, 298 K) of compound **PyCEPt-1**.

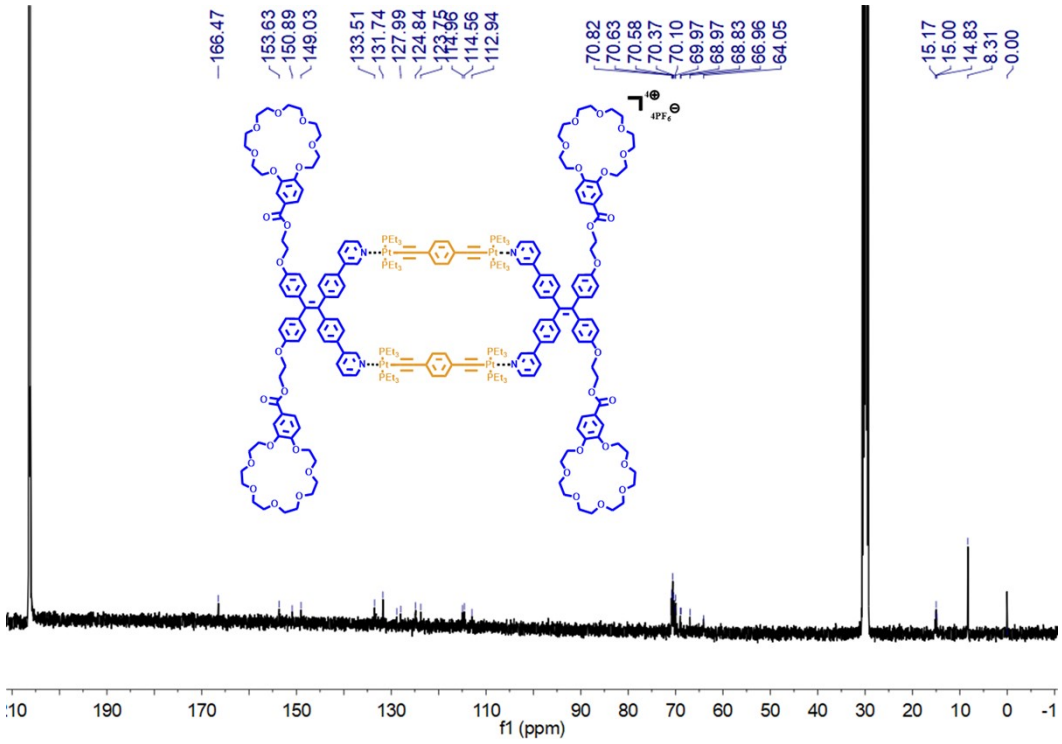

Fig. S28 ^{13}C NMR spectrum (100 MHz, acetone-d_6, 298 K) of compound **PyCEPt-1**.

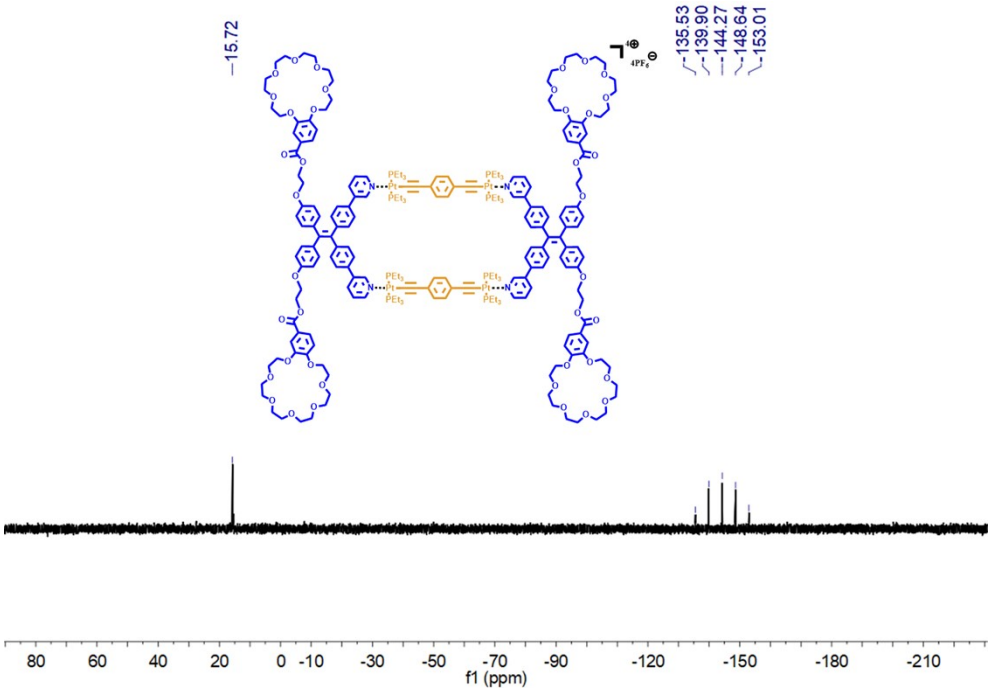

Fig. S29 ^{31}P NMR spectrum (162 MHz, acetone-d_6, 298 K) of compound **PyCEPt-1**.

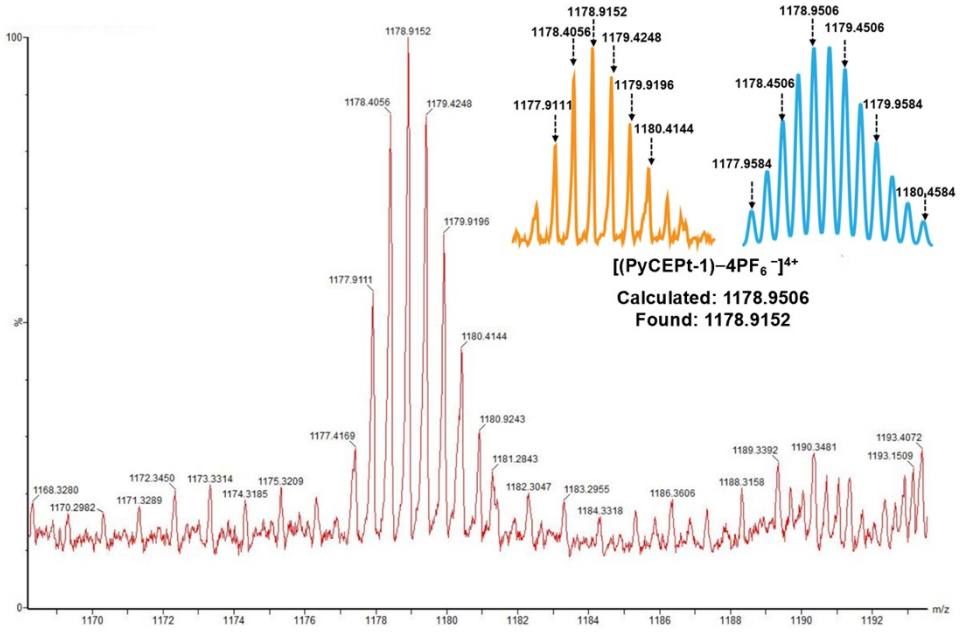

Fig. S30 ESI-TOF-MS spectrum of **PyCEPt-1**. The inset: ESI-TOF-MS spectra of [(**PyCEPt-1**)−4PF_6^-]$^{4+}$: experimental data (yellow) and calculated result (blue).

Synthesis of metallacycle PyPt

Compounds **Py** (30 mg, 0.06 mmol) and **M** (76 mg, 0.06 mmol) were weighed separately and dissolved in dry DCM (1 mL). The self-assembly was done by slowly adding compound **M** to the solution of compound **Py**, and the whole reaction mixture was stirred for 24 hours at room temperature. The solvent was evaporated under nitrogen flow, and the self-assembled metallacycle was isolated and recrystallized with DCM-ethyl ether. The precipitated residue was redissolved in

dry DCM (2.0 mL) and filtered through glass wool. The solvent was removed by nitrogen flow, and the compound was further dried under vacuum at room temperature to yield compound **PyPt** as a brown powder (70.0 mg, 0.04 mmol, yield: 70%). ^{1}H NMR (400 MHz, $CDCl_3$, 298 K) δ 9.07 (s, 4H), 8.75 (d, J = 3.2 Hz, 4H), 8.11 (d, J = 6.1 Hz, 4H), 7.93 – 7.88 (m, 4H), 7.50 (s, 8H), 7.32 (s, 8H), 7.23 (dd, J = 4.8, 1.4 Hz, 12H), 7.21 – 7.13 (m, 16H), 1.66 (m, 48H), 1.22 – 1.13 (m, 72H). ^{31}P NMR (162 MHz, $CDCl_3$, 298 K) δ 12.47 (s, ^{195}Pt satellites, $^{1}J_{Pt\text{-}P}$ = 2270 Hz).

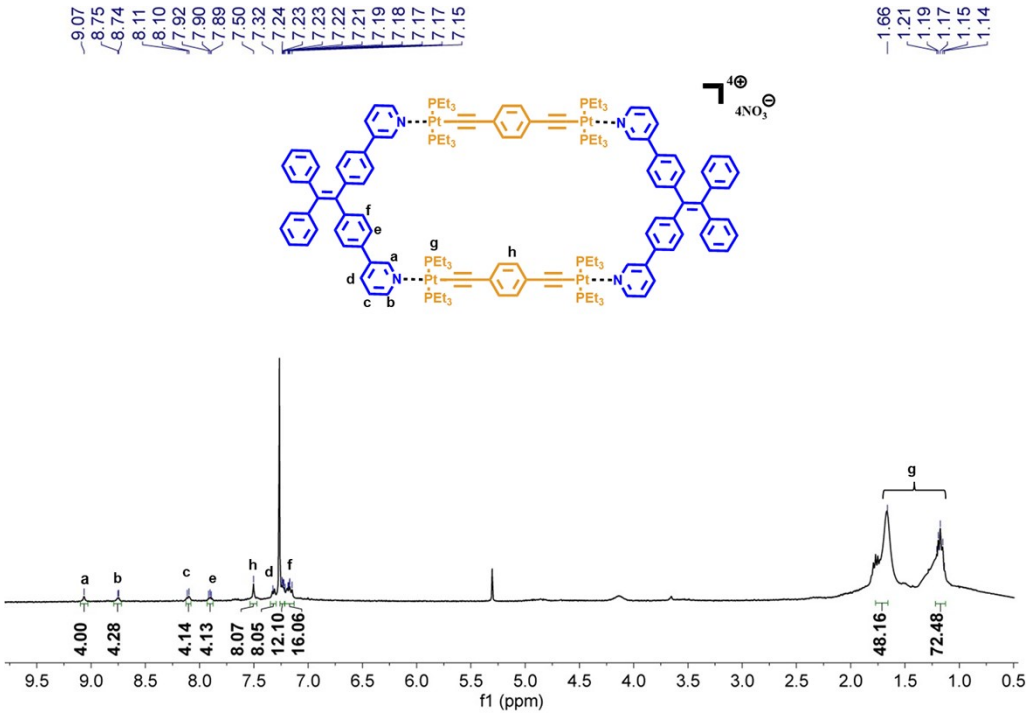

Fig. S31 ^{1}H NMR spectrum (400 MHz, $CDCl_3$, 298 K) of compound **PyPt**.

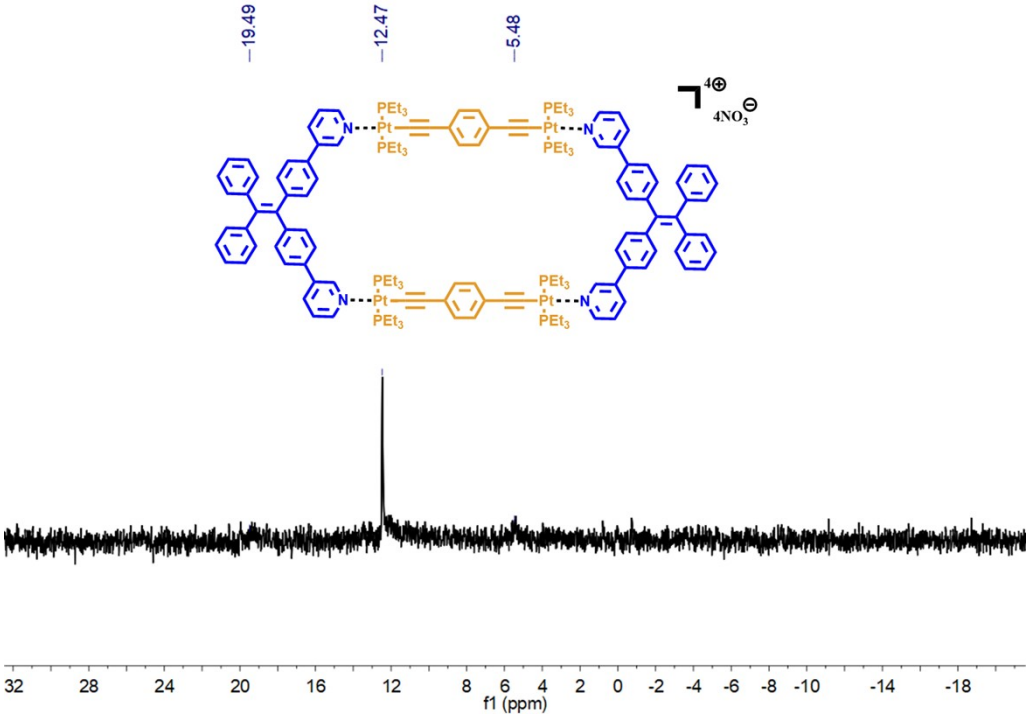

Fig. S32 ^{31}P NMR spectrum (162 MHz, $CDCl_3$, 298 K) of compound **PyPt**.

Compound **PyPt** (12.1 mg, 0.004 mmol) was dissolved in 1 mL of DMF in a 10 mL vial, followed by the addition of a saturated aqueous solution of KPF_6 (2 mL) to precipitate the product. The reaction mixture was centrifuged; the resulting solid was washed repeatedly with deionized water and vacuum-dried at room temperature, yielding the yellow precipitate **PyPt-1**. ^{1}H NMR (400 MHz, acetone-d_6, 298 K) δ 9.18 (s, 2H), 9.08 (s, 2H), 8.96 (d, J = 5.4 Hz, 4H), 8.42 (d, J = 7.9 Hz, 2H), 8.35 (d, J = 8.1 Hz, 2H), 7.92 – 7.84 (m, 4H), 7.64 (d, J = 8.3 Hz, 2H), 7.57 (d, J = 8.3 Hz, 4H), 7.35 – 7.26 (m, 8H), 7.24 – 7.18 (m, 20H), 7.15 – 7.08 (m, 10H), 2.02 – 1.90 (m, 48H), 1.29 – 1.15 (m, 72H). ^{31}P NMR (162 MHz, acetone-d_6, 298 K) δ 15.71 (s, ^{195}Pt satellites, $^{1}J_{Pt\text{-}P}$ = 2334 Hz). ^{13}C NMR (100 MHz, acetone-d_6, 298 K) δ 153.39, 151.75, 146.45, 144.90, 140.62, 139.65, 134.97, 133.86, 132.72, 132.54, 129.96, 129.73, 128.78, 128.56, 15.97, 15.80, 15.63, 9.10, 9.07. DOSY NMR (400 MHz, acetone-d_6, 298 K) spectrum was recorded for **PyPt-1**, revealing a diffusion coefficient (D) of 3.71 × 10^{-6} cm^2/sec. ESI-TOF-MS: calculated for [(**PyPt-1**)−4PF_6^-]$^{4+}$, 736.7662; found, 736.7386.

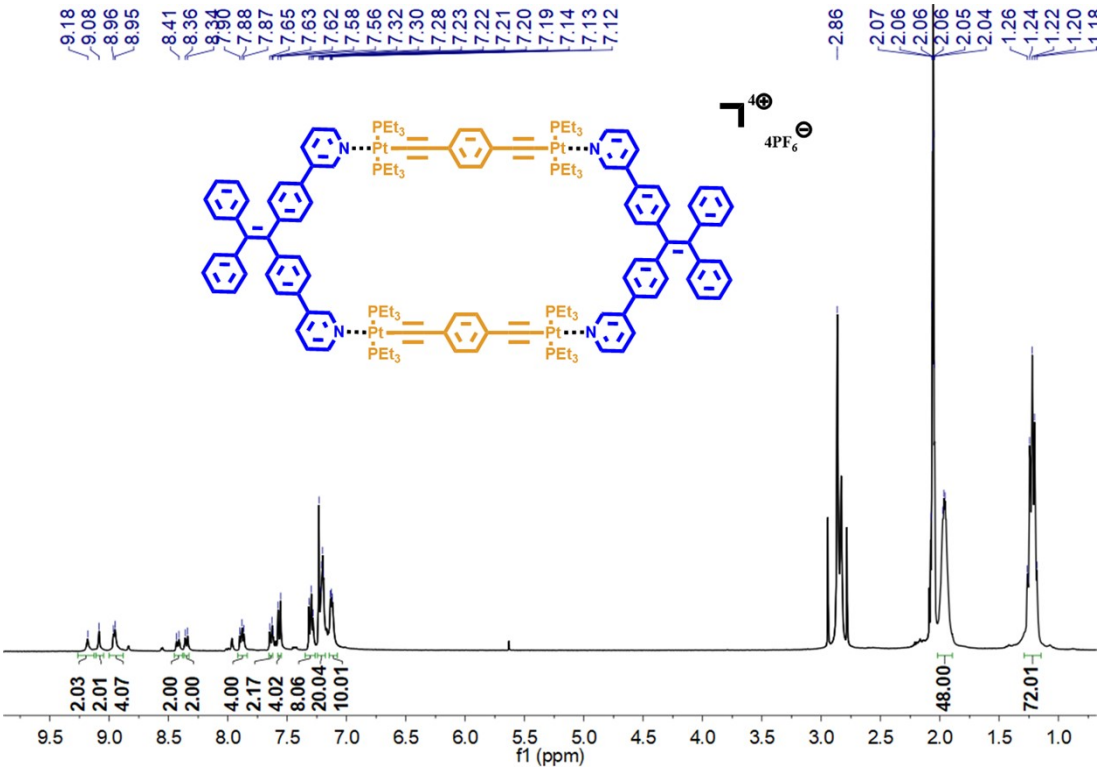

Fig. S33 ^{1}H NMR spectrum (400 MHz, acetone-d_6, 298 K) of compound **PyPt-1**.

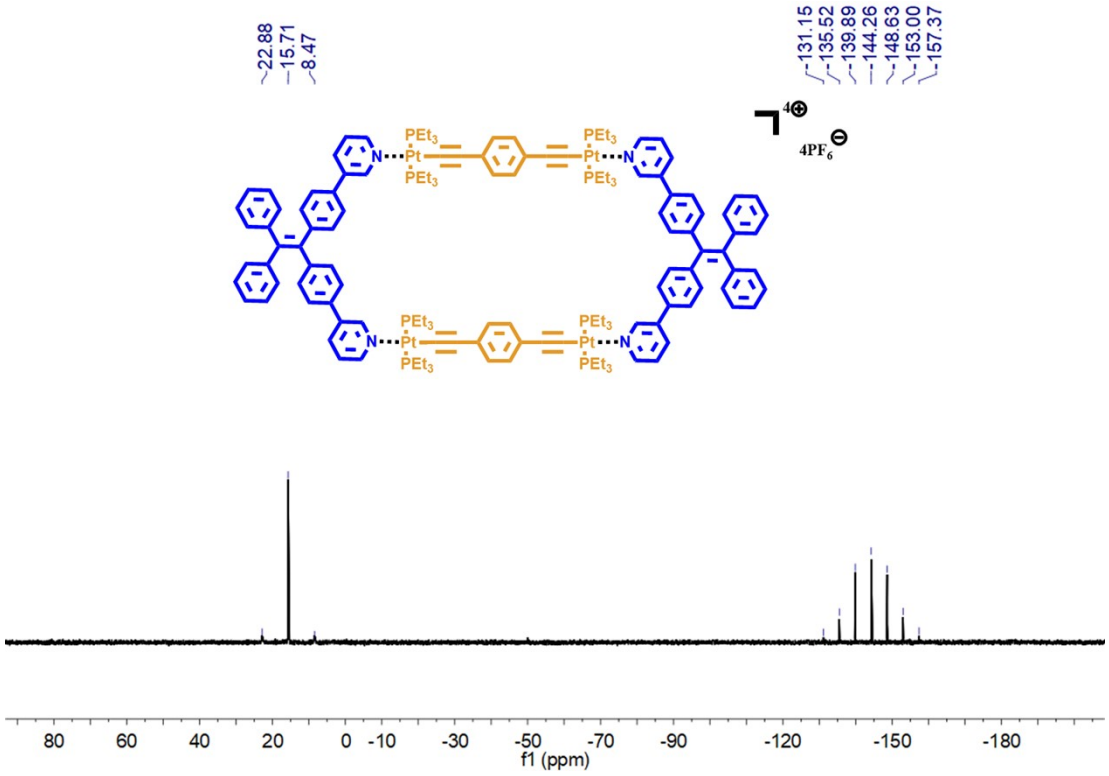

Fig. S34 ^{31}P NMR spectrum (162 MHz, acetone-d_6, 298 K) of compound **PyPt-1**.

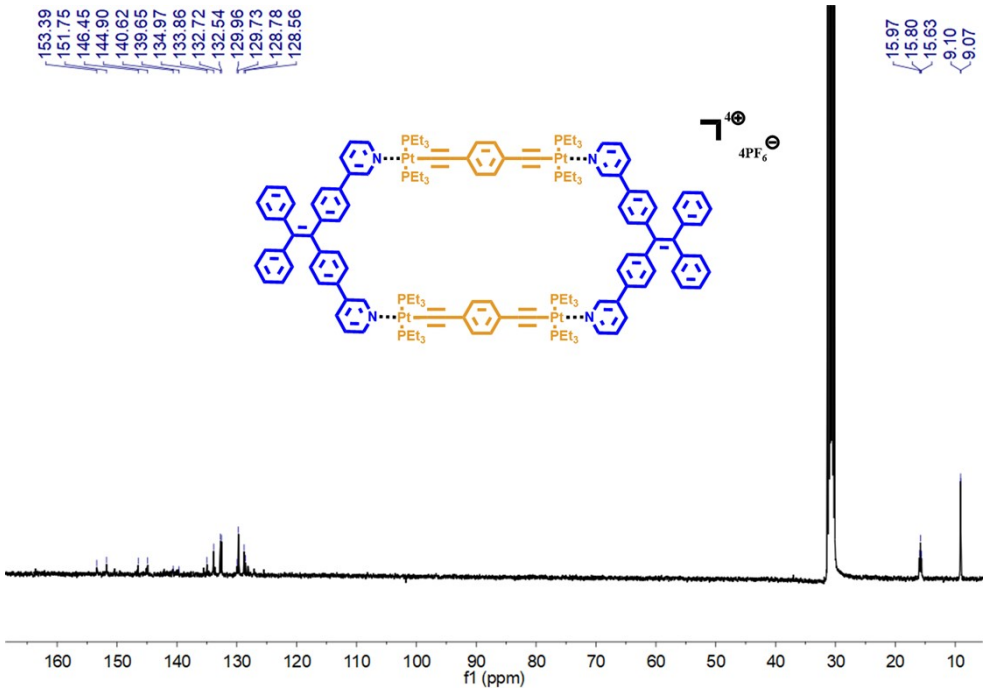

Fig. S35 ^{13}C NMR spectrum (100 MHz, acetone-d_6, 298 K) of compound **PyPt-1**.

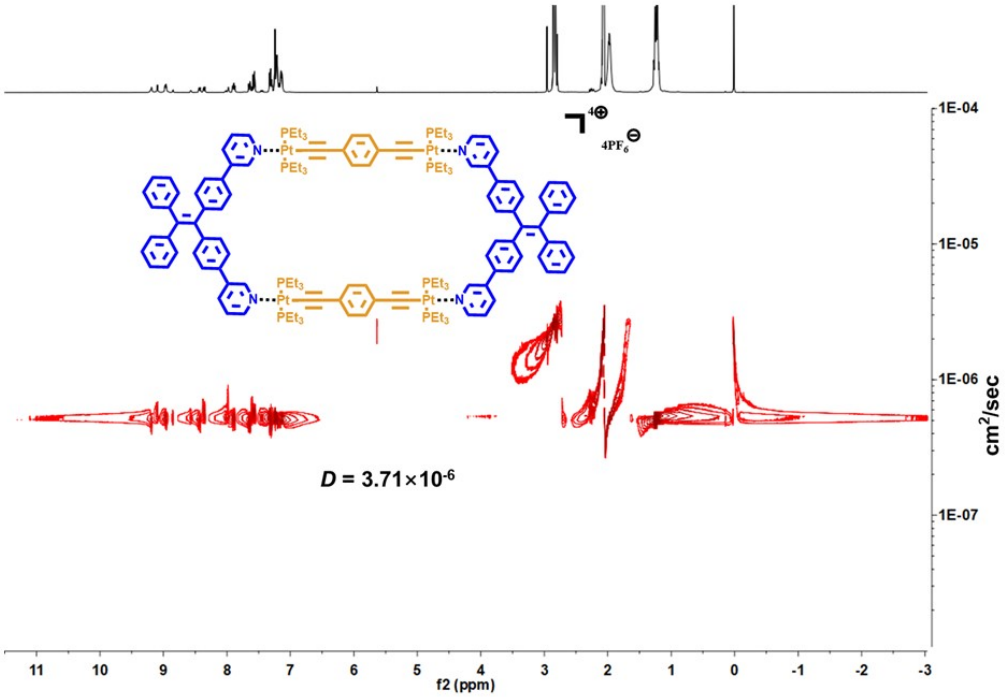

Fig. S36 DOSY NMR spectrum (400 MHz, acetone-d_6, 298 K) of compound **PyPt-1**.

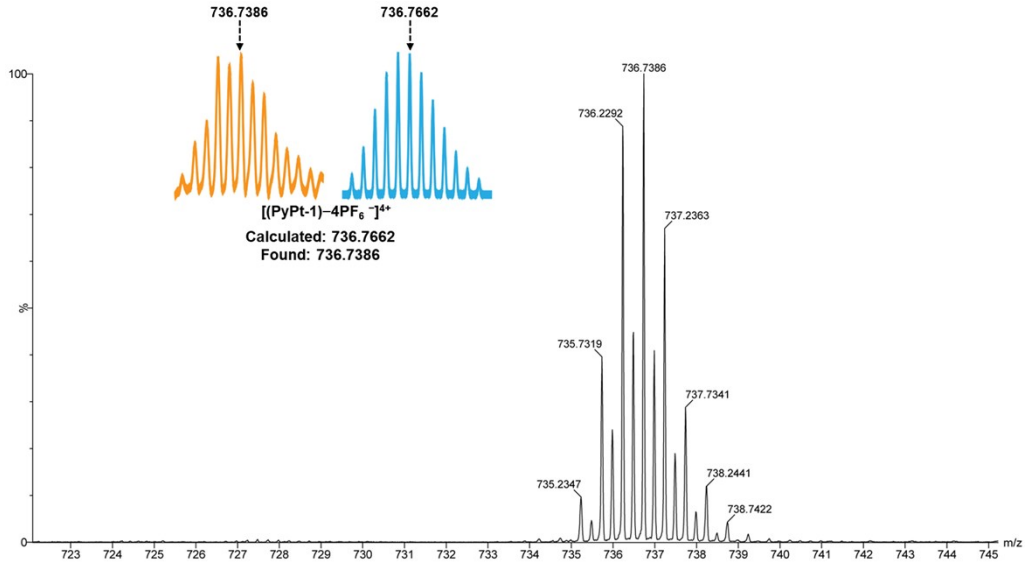

Fig. S37 ESI-TOF-MS spectrum of **PyPt-1**. The inset: ESI-TOF-MS spectra of [(**PyPt-1**)–4PF_6^-]$^{4+}$: experimental data (yellow) and calculated result (blue).

3. AIE properties of compounds PyCE and PyCEPt

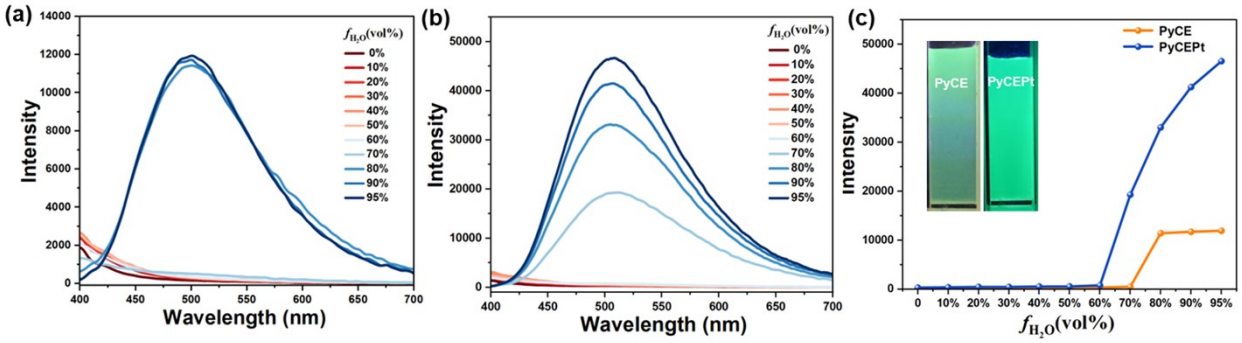

Fig. S38 Fluorescence spectra of (a) **PyCE** and (b) **PyCEPt** in the H_2O/CH_3CN mixture with different H_2O contents (0-95%). (c) Plot of maximum emission intensity of **PyCE** and **PyCEPt** (λ_{em} = 510 nm). The inset: fluorescence images of **PyCE** (left) and **PyCEPt** (right) in the H_2O/CH_3CN (95/5, *v/v*) under UV-light irradiation at 365 nm. [**PyCE**] = [**PyCEPt**] = 2×10^{-5} M.

4. Fluorescence quantum yields and fluorescence lifetime measurements

To further verify the occurrence of the light-harvesting process, fluorescence quantum yields and fluorescence decay experiments were performed. The fluorescence lifetimes were fitted as a double exponential decay. The results showed that the lifetime of the nanoparticles gradually decreased with the loading of dyes, suggesting that the **PyCEPt⊃G** assembly could serve as an efficient light-harvesting system to transfer the captured energy first to ESY and then to SR101.

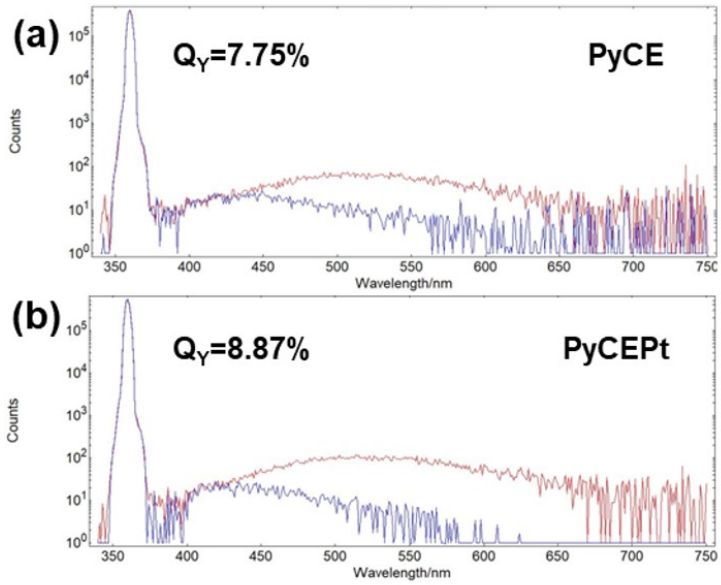

Fig. S39 Absolute fluorescence quantum yields ($\Phi_{f(Abs)}$) of (a) **PyCE** and (b) **PyCEPt** upon excitation at 360 nm in aqueous solution. [**PyCE**] = [**PyCEPt**] = 2×10^{-5} M.

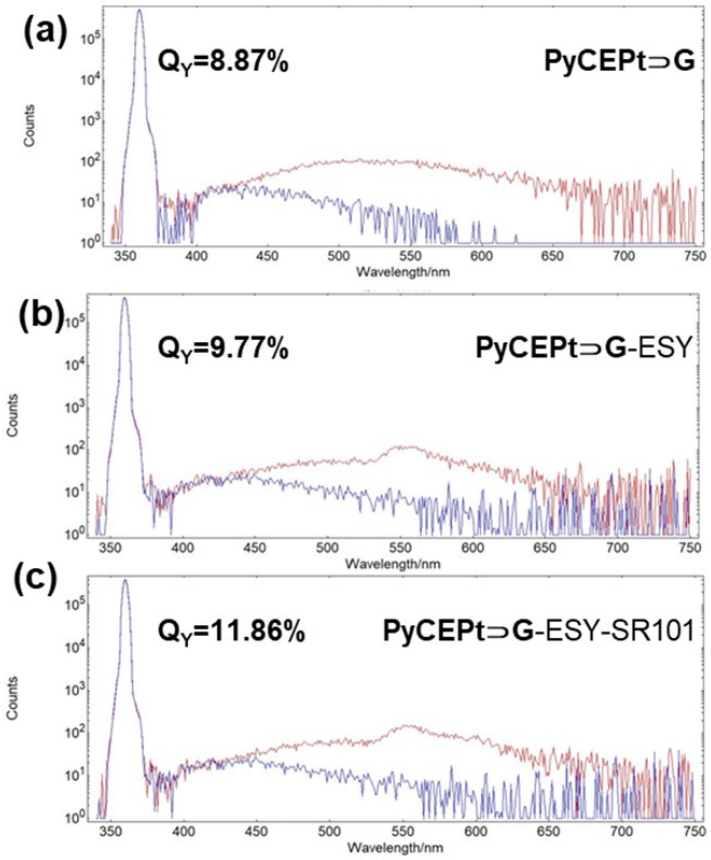

Fig. S40 Absolute fluorescence quantum yields ($\Phi_{f(Abs)}$) of (a) **PyCE⊃G** assembly, (b) **PyCEPt**-ESY assembly, and (c) **PyCEPt**-ESY-SR101 assembly upon excitation at 360 nm in aqueous solution. [**PyCEPt**] = 2 × 10^{-5} M, [**G**] = 8 × 10^{-5} M, [ESY] = 1 × 10^{-7} M, [SR101] = 1 × 10^{-7} M.

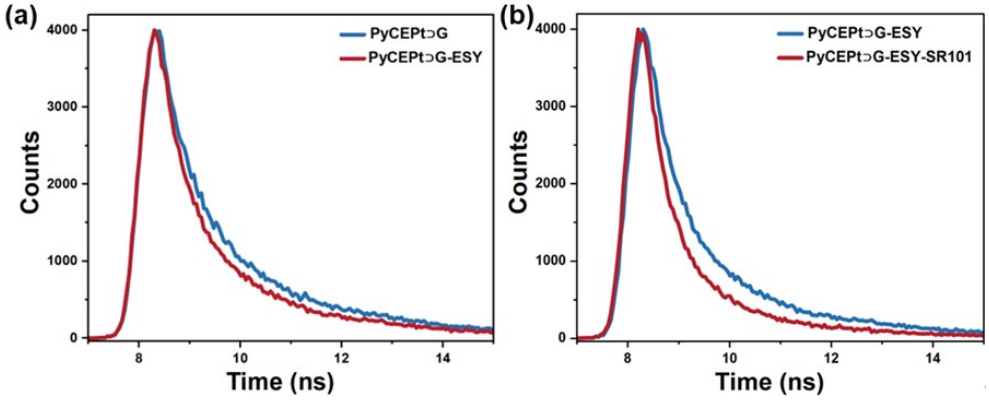

Fig. S41 Fluorescence decay profiles of (a) **PyCEPt⊃G** and **PyCEPt⊃G**-ESY (200:1) assembly monitored at λ_{ex} = 510 nm and (b) **PyCEPt⊃G**-ESY (200:1) and **PyCEPt⊃G**-ESY-SR101 (200:1:1) assembly monitored at λ_{ex} = 550 nm in H_2O/CH_3CN (95/5, *v/v*). [**PyCEPt**] = 2 × 10^{-5} M, [**G**] = 8 × 10^{-5} M, [ESY] = 1 × 10^{-7} M, [SR101] = 1 × 10^{-7} M.

Table S1 Fluorescence lifetimes of **PyCEPt⊃G** assembly, **PyCEPt⊃G**-ESY (200:1) assembly, and **PyCEPt⊃G**-ESY-SR101 (200:1:1) assembly upon excitation at 360 nm. [**PyCEPt**] = 2×10^{-5} M, [**G**] = 8×10^{-5} M, [ESY] = 1×10^{-7} M, [SR101] = 1×10^{-7} M.

Sample	τ_1 /ns	Rel/%	τ_2 /ns	Rel/%	τ /ns	χ^2
PyCEPt⊃G	0.8348	43.13	3.1053	56.87	2.1260	0.8684
PyCEPt⊃G-ESY	0.7021	44.66	2.7164	55.34	1.8167	0.7636
PyCEPt⊃G-ESY-SR101	0.5722	56.72	2.3394	43.28	1.3370	0.7280

5. Study on the host-guest interactions

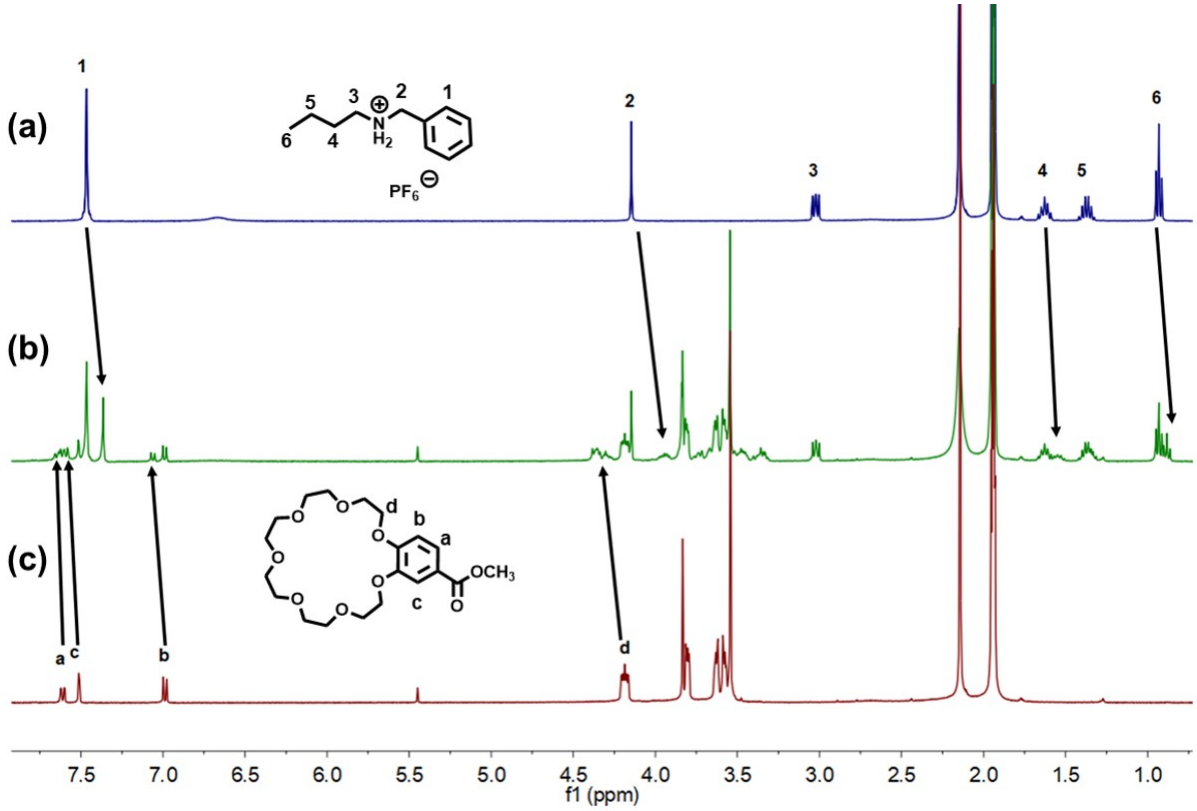

Fig. S42 ^{1}H NMR (400 MHz, CD_3CN, 298 K) spectra: (a) $\mathbf{G_M}$ (4.0 mM), (b) $\mathbf{H_M}$ (4.0 mM) + $\mathbf{G_M}$ (4.0 mM), and (c) $\mathbf{H_M}$ (4.0 mM).

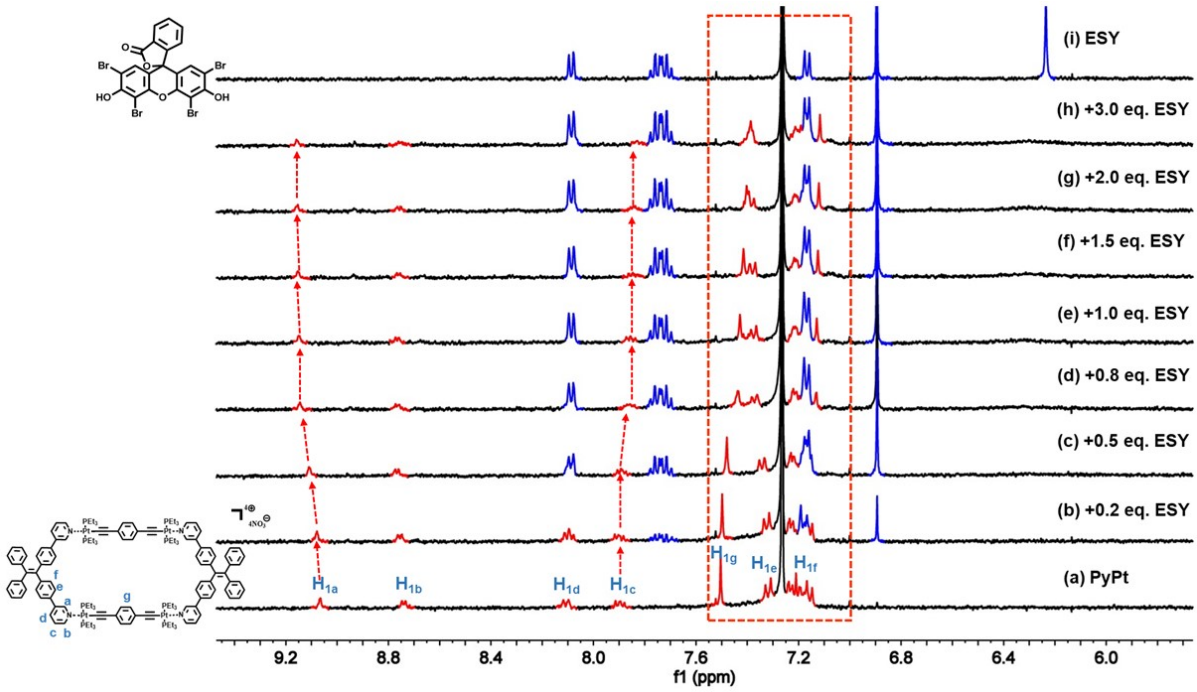

Fig. S43 ^{1}H NMR spectra of **PyPt** (400 MHz, $CDCl_3$, 298 K) in the presence of increasing equivalents of ESY; from (a) to (h): 0, 0.2, 0.5, 0.8, 1.0, 1.5, 2.0, and 3.0 equivalents; i) free ESY.

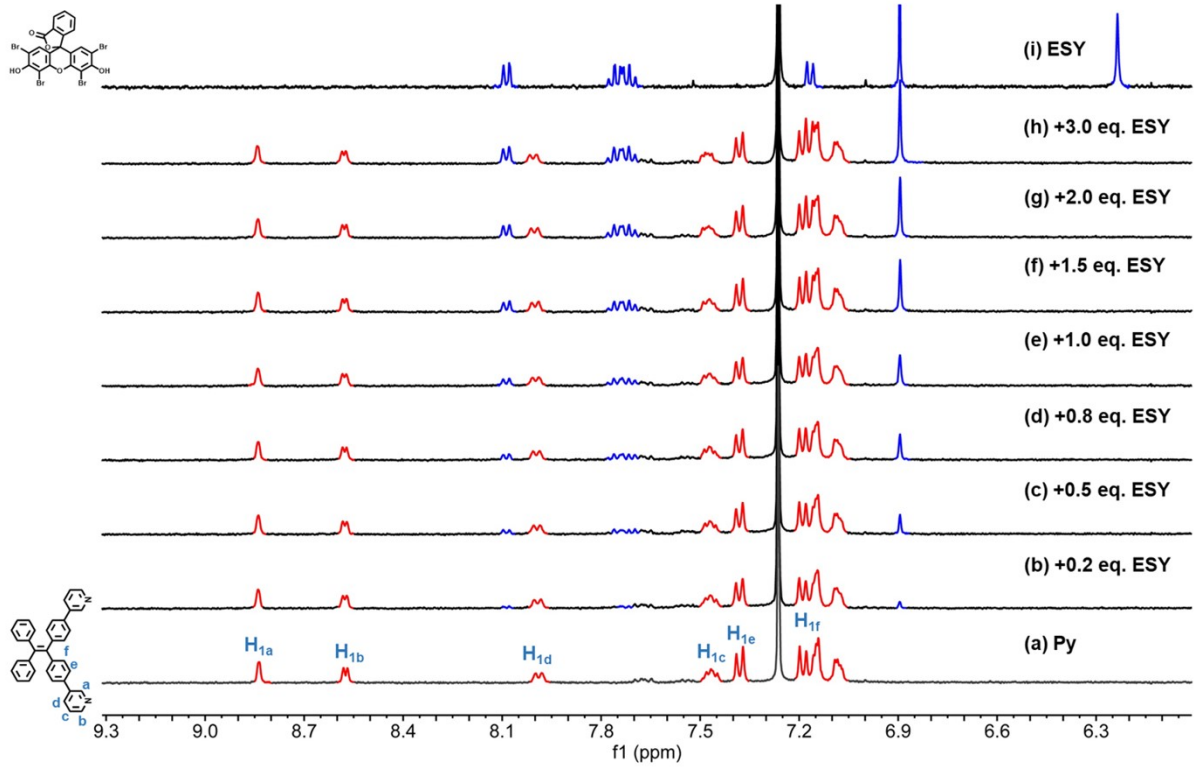

Fig. S44 ^{1}H NMR spectra of **Py** (400 MHz, $CDCl_3$, 298 K) in the presence of increasing equivalents of ESY; from (a) to (h): 0, 0.2, 0.5, 0.8, 1.0, 1.5, 2.0 and 3.0 equivalents; i) free ESY.

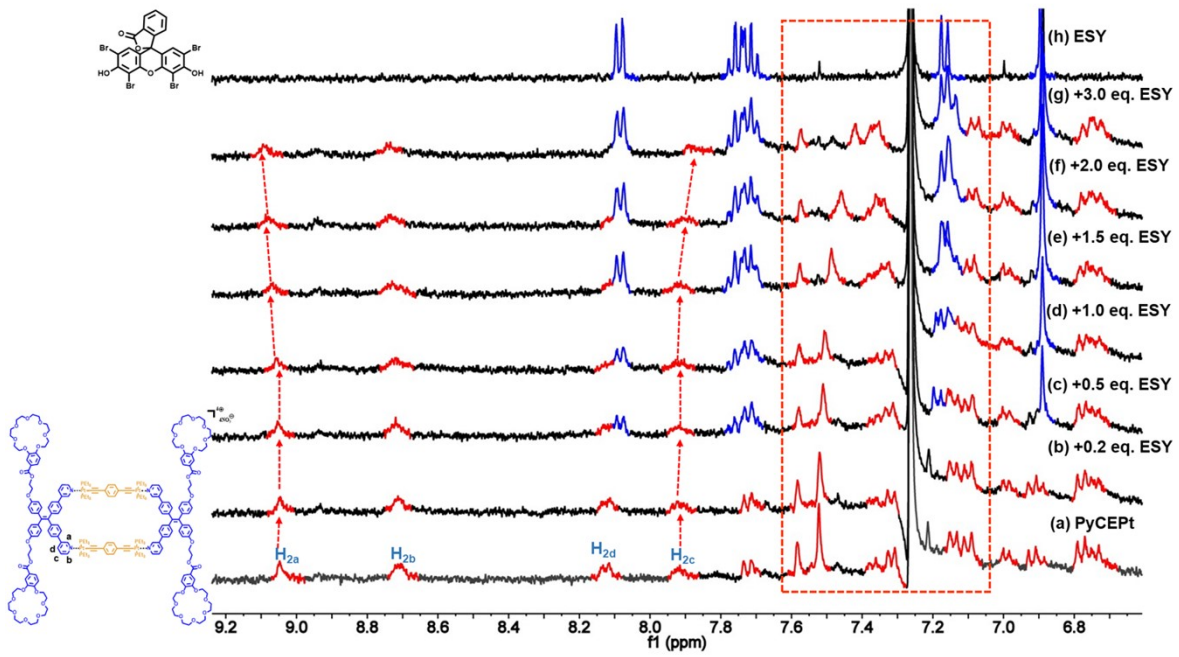

Fig. S45 ^{1}H NMR spectra of **PyCEPt** (400 MHz, $CDCl_3$, 298 K) in the presence of increasing equivalents of ESY; from (a) to (g): 0, 0.2, 0.5, 1.0, 1.5, 2.0 and 3.0 equivalents; h) free ESY.

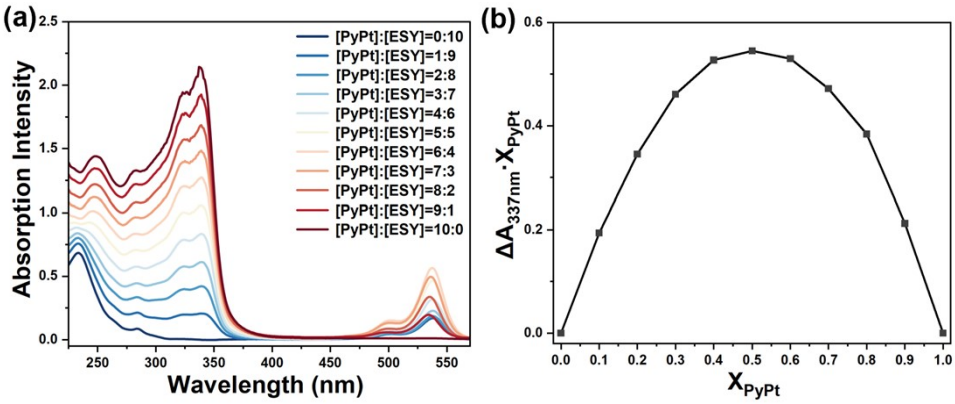

Fig. S46 UV-vis absorption spectra of **PyPt**⊃ESY complex and Job's plot of the 1:1 binding ratio between **PyPt** and ESY ([**PyPt**] + [ESY] = 4.0×10^{-5} M, solvent: $CHCl_3$).

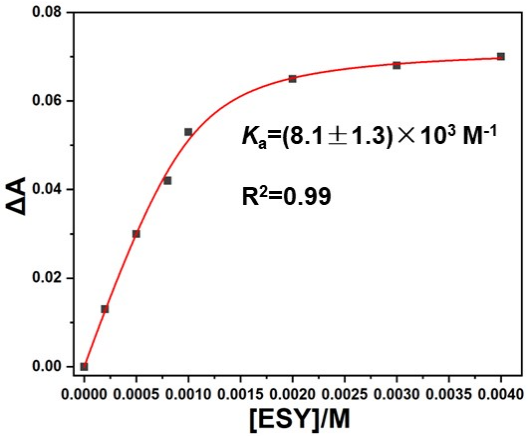

Fig. S47 The association constant (K_a) value of the complex between **PyPt** (1.0×10^{-3} M, solvent: $CDCl_3$) and ESY (0-4.0×10^{-3} M, solvent: $CDCl_3$).

6. Study on the FRET process

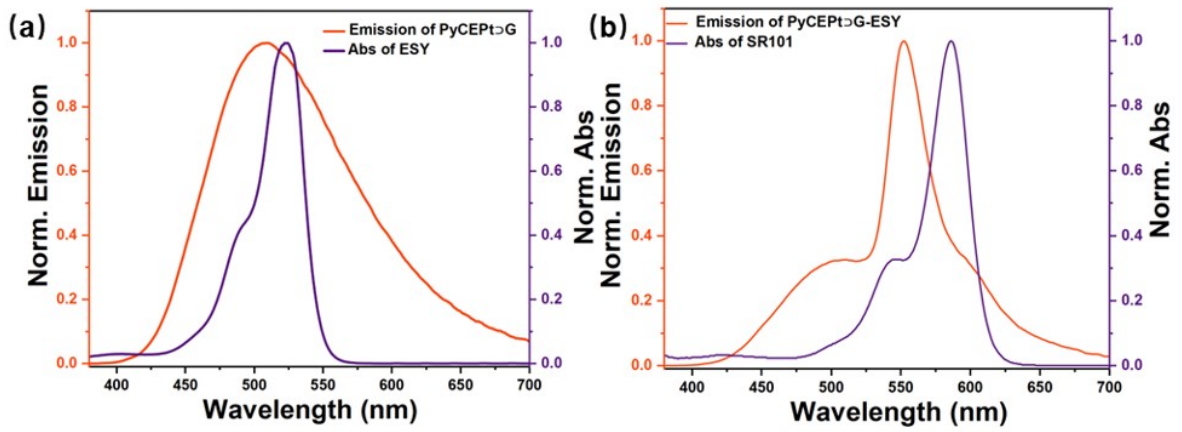

Fig. S48 Normalized emission spectrum of (a) **PyCEPt⊃G** assembly upon excitation at 360 nm and normalized absorption spectrum of ESY in aqueous media; (b) Normalized emission spectrum of **PyCEPt⊃G**-ESY assembly upon excitation at 360 nm and normalized absorption spectrum of SR101 in aqueous media.

7. Energy-transfer efficiency and antenna effect calculations

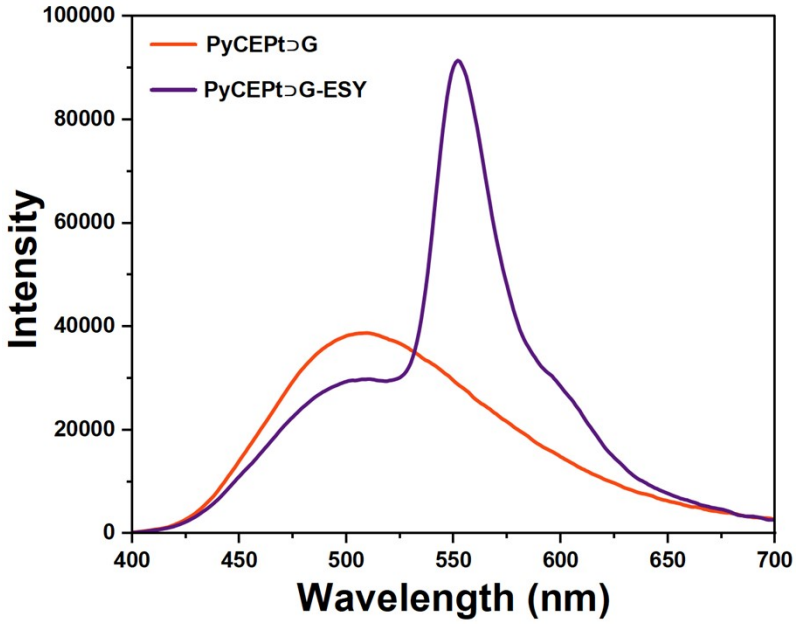

Fig. S49 Fluorescence spectra of **PyCEPt⊃G** and **PyCEPt⊃G**-ESY assembly upon excitation at 360 nm. [**PyCEPt**] = 2×10^{-5} M, [**G**] = 8×10^{-5} M, [ESY] = 1×10^{-7} M.

Energy-transfer efficiency (Φ_{ET}) was calculated from excitation fluorescence spectra through the equation S1[8]:

$$\mathbf{\Phi_{ET} = 1 - I_{DA} / I_D} \text{ (eq. S1)}$$

Where I_{DA} and I_D are the fluorescence intensities of the emission of **PyCEPt⊃G**-ESY assembly (donor and acceptor) and **PyCEPt⊃G** assembly (donor), respectively when excited at 360 nm.

The energy-transfer efficiency (Φ_{ET}) was calculated as 22.98% in aqueous media, measured under the conditions of [**PyCEPt**] = 2 × 10^{-5} M, [**G**] = 8 × 10^{-5} M, [ESY] = 1 × 10^{-7} M, and λ_{ex} = 360 nm.

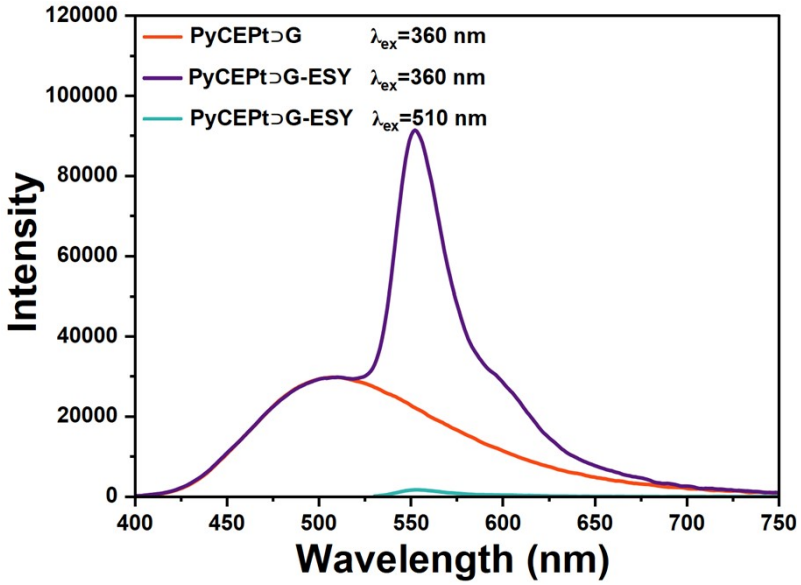

Fig. S50 Fluorescence spectra of **PyCEPt⊃G**-ESY in aqueous media (purple line), blue line (acceptor emission, λ_{ex} = 510 nm). The red line represents the fluorescence spectrum of **PyCEPt⊃G**, which was normalized according to the fluorescence intensity at 510 nm of the purple line. [**PyCEPt**] = 2 × 10^{-5} M, [**G**] = 8 × 10^{-5} M, [ESY] = 1 × 10^{-7} M.

The antenna effect (AE) was calculated based on the excitation spectra using equation S2:

$$\mathbf{AE = (I_{DA,360} - I_{D,360}) / I_{DA,510}} \text{ (eq. S2)}$$

Where $I_{DA,360}$ and $I_{DA,510}$ are the fluorescence intensities at 550 nm with the excitation of the donor at 360 nm and the direct excitation of the acceptor at 510 nm, respectively. $I_{D,360}$ is the fluorescence intensity at 550 nm of the **PyCEPt⊃G** assembly, which was normalized with the **PyCEPt⊃G**-ESY assembly at 510 nm.

The antenna effect value was calculated as 41.13 in aqueous media, measured under the conditions of [**PyCEPt**] = 2 × 10^{-5} M, [**G**] = 8 × 10^{-5} M, and [ESY] = 1 × 10^{-7} M.

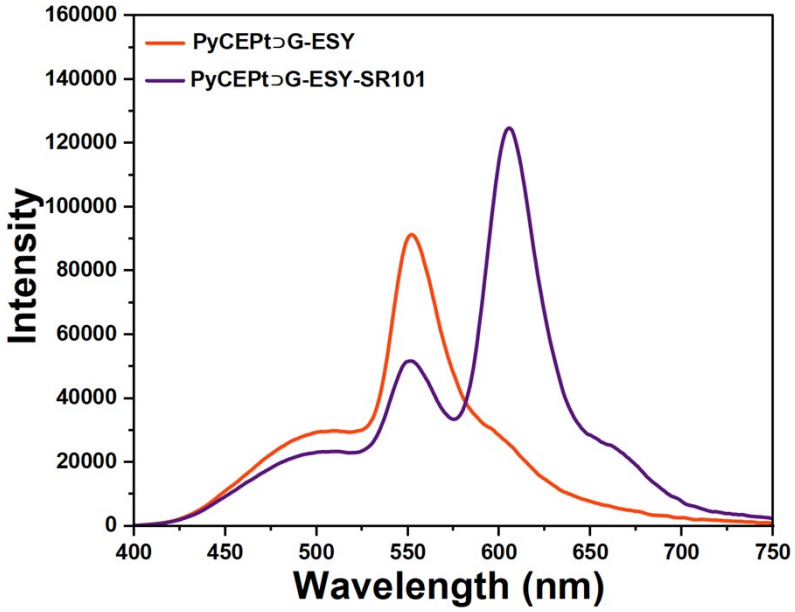

Fig. S51 Fluorescence spectra of **PyCEPt⊃G**-ESY and **PyCEPt⊃G**-ESY-SR101 assembly upon excitation at 360 nm. [**PyCEPt**] = 2 × 10^{-5} M, [**G**] = 8 × 10^{-5} M, [ESY] = 1 × 10^{-7} M, [SR101] = 1 × 10^{-7} M.

The energy-transfer efficiency (Φ_{ET}) was calculated as 42.82% in aqueous media, measured under the conditions of [**PyCEPt**] = 2 × 10^{-5} M, [**G**] = 8 × 10^{-5} M, [ESY] = 1 × 10^{-7} M, [SR101] = 1 × 10^{-7} M, and λ_{ex} = 360 nm.

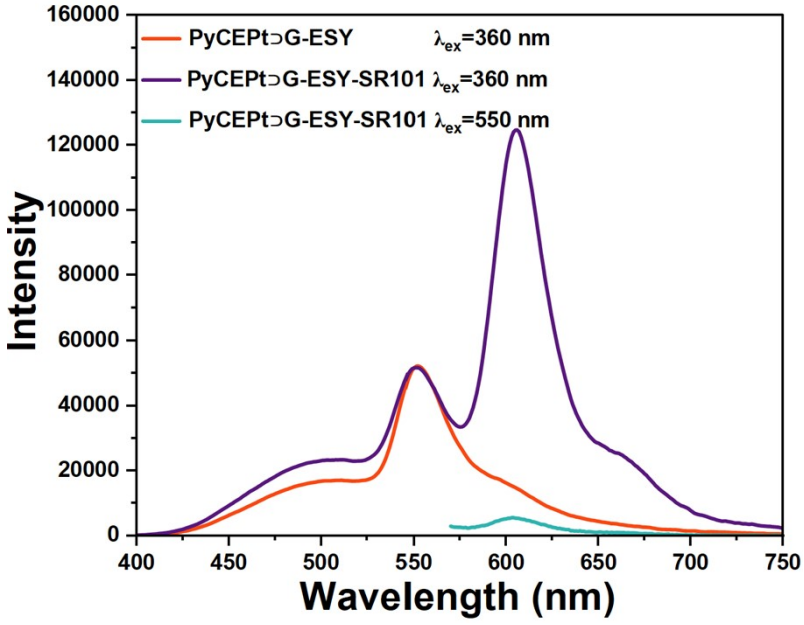

Fig. S52 Fluorescence spectra of **PyCEPt⊃G**-ESY-SR101 in aqueous media (purple line), blue line (acceptor emission, λ_{ex} = 550 nm). The red line represents the fluorescence spectrum of **PyCEPt⊃G**-ESY, which was normalized according to the fluorescence intensity at 550 nm of the purple line. [**PyCEPt**] = 2 × 10^{-5} M, [**G**] = 8 × 10^{-5} M, [ESY] = 1 × 10^{-7} M, [SR101] = 1 × 10^{-7} M.

The antenna effect value was calculated as 20.03 in aqueous media, measured under the conditions of [**PyCEPt**] = 2 × 10^{-5} M, [**G**] = 8 × 10^{-5} M, [ESY] = 1 × 10^{-7} M, and [SR101] = 1 × 10^{-7} M.

8. Investigation of $^1O_2$ and $O_2^{\bullet-}$ generation

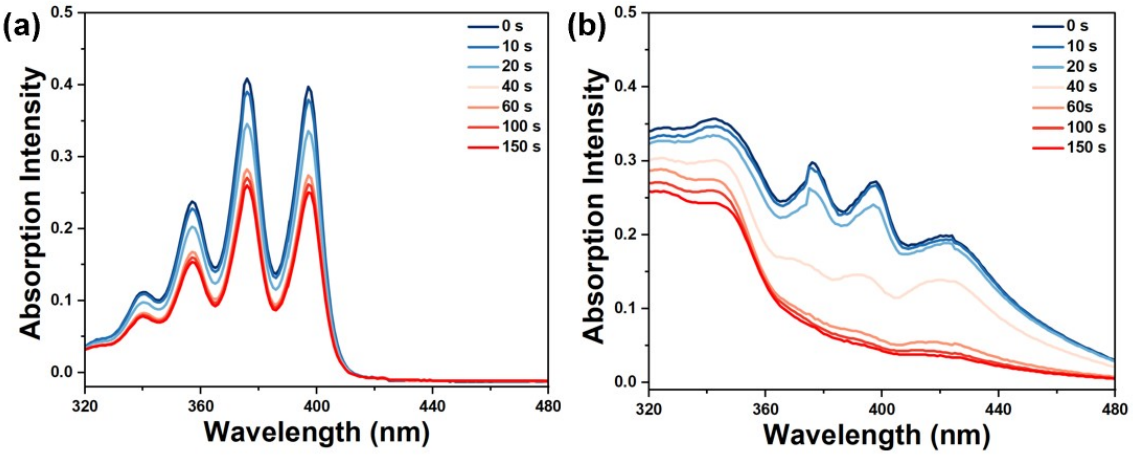

Fig. S53 UV-vis absorption spectra of ABDA after irradiation for varying durations (365 nm, 6 W): (a) control: aqueous solution of ABDA without any additives; (b) aqueous solution of ABDA with the addition of **PyCEPt⊃G**-ESY-SR101. [**PyCEPt**] = 2 × 10^{-5} M, [**G**] = 8 × 10^{-5} M, [ESY] = 1 × 10^{-7} M, [SR101] = 1 × 10^{-7} M, and [**ABDA**] = 4 × 10^{-5} M.

Nitro blue tetrazolium (NBT) is widely utilized as a probe for the detection of $O_2^{\bullet-}$, which forms formazan (a blue/violet colored precipitate) upon capturing $O_2^{\bullet-}$.[9] Herein, upon the addition of **PyCEPt⊃G**-ESY-SR101 and thioanisole into NBT solution, the formation of blue precipitate could be observed after irradiation.

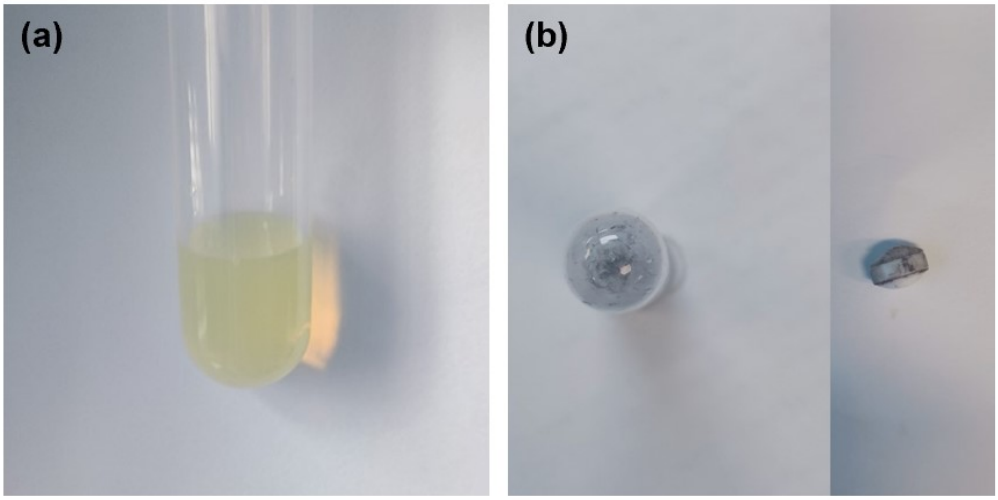

Fig. S54 (a) Photograph of aqueous solution of NBT; (b) Photograph of precipitate formazan after the addition of **PyCEPt⊃G**-ESY-SR101 and thioanisole under irradiation with a 6 W, 365 nm UV light for 3 hours. [**PyCEPt**] = 1 × 10^{-6} M, [**G**] = 4 × 10^{-6} M, [ESY] = 5 × 10^{-8} M, [SR101] = 5 × 10^{-8} M, and NBT (4 mg, 0.004 mmol).

9. Photographs of the changes of reaction solutions with different photocatalytic

During the photooxidation process of thioanisole, we observed that the fluorescence color in all systems gradually faded. However, the degree of color weakening in the **PyCEPt⊃G**-ESY-SR101 system was significantly less than that in other systems, indicating that the structural confinement provided by the supramolecular cavity effectively suppresses dye photodegradation.

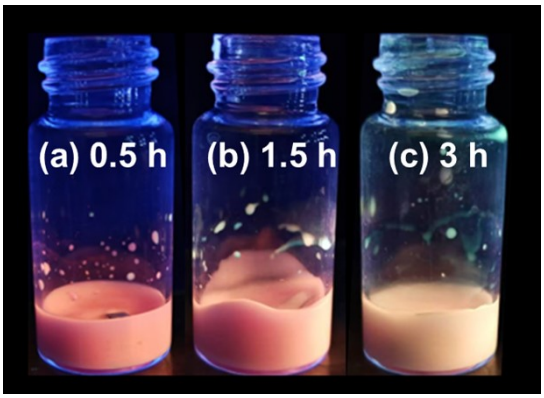

Fig. S55 Photographs of photocatalytic oxidation of thioanisole by **PyCEPt⊃G**-ESY-SR101 under 6 W UV light at 365 nm over time: (a) 0.5 h, (b) 1.5 h and (c) 3 h.

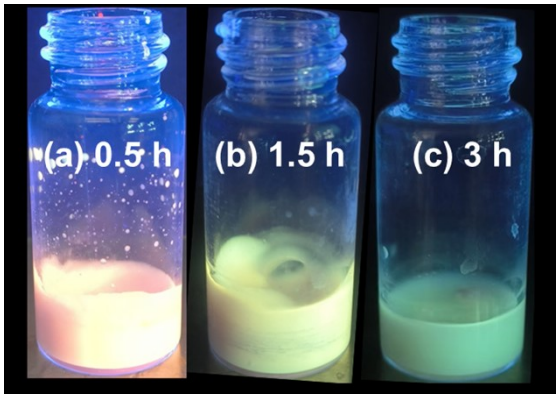

Fig. S56 Photographs of photocatalytic oxidation of thioanisole by **PyCE⊃G**-ESY-SR101 under 6 W UV light at 365 nm over time: (a) 0.5 h, (b) 1.5 h and (c) 3 h.

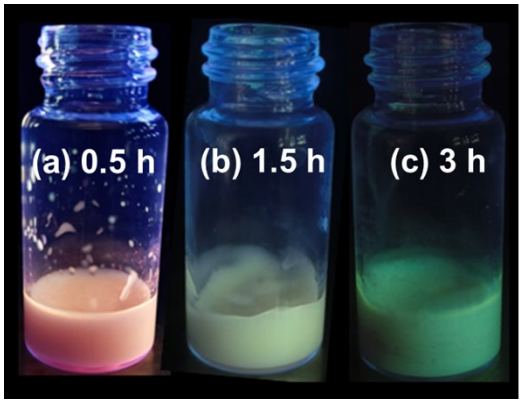

Fig. S57 Photographs of photocatalytic oxidation of thioanisole by **PyPt-1**-ESY-SR101 under 6 W UV light at 365 nm over time: (a) 0.5 h, (b) 1.5 h and (c) 3 h.

10. PyCEPt⊃G-ESY-SR101 system for the photocatalytic reaction in aqueous medium

In the model **PyPt-1**-ESY-SR101 system, although the metallacycle endowing it with the capacity to bind ESY, the absence of the crown ether cavity prevents its formation of a supramolecular network with the guest molecule. The molecular aggregation is restricted, which subsequently results in a low energy transfer efficiency between the host and the dye. Conversely,, in the non-coordinating **PyCE⊃G**-ESY-SR101 system, the absence of the metallacycle structure prevents its coordination with ESY. It is challenging to reduce the FRET distance, and ESY remains in an exposed-to-light state for a long period, thereby causing inevitable photobleaching. Therefore, the **PyCEPt⊃G**-ESY-SR101 system achieves a shorter FRET distance and effective suppression of dye photobleaching through the interaction between the metallacycle and ESY. Simultaneously, it forms a supramolecular network via host-guest interaction in the crown ether to enhance molecular aggregation. This synergy facilitates energy transfer and photocatalytic efficiency, leading to a significant improvement in catalytic yields.

Table S2 Different reaction conditions for the photooxidation of thioanisole.[a]

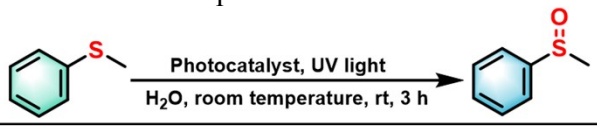

Entry	Conditions	Light irradiation	Atmosphere	Yield[b]
1	None	Yes	Air	15%
2	ESY+SR101	Yes	Air	40%
3	**PyCEPt⊃G**	Yes	Air	31%
4	**PyCEPt⊃G**-ESY	Yes	Air	72%
5	**PyCEPt⊃G**-SR101	Yes	Air	38%
6	**PyCE⊃G**-ESY-SR101	Yes	Air	63%
7	**PyPt-1**-ESY-SR101	Yes	Air	68%
8	**PyCEPt⊃G**-ESY-SR101	Yes	Air	87%
9	**PyCEPt⊃G**-ESY-SR101[c]	Yes	Nitrogen	Trace
10	**PyCEPt⊃G**-ESY-SR101[d]	No	Air	No reaction

[a] Reaction conditions: thioanisole (0.1 mmol, 1 equiv.), **PyCEPt⊃G**-ESY-SR101 assembly solution (1.0 mol%, 2 mL). 6 W UV light, room temperature, 3 h; [b] Isolated yields; [c] N_2 atmosphere; [d] Without light irradiation.

Table S3 Photooxidation reactions of thioanisole derivatives.[a,b]

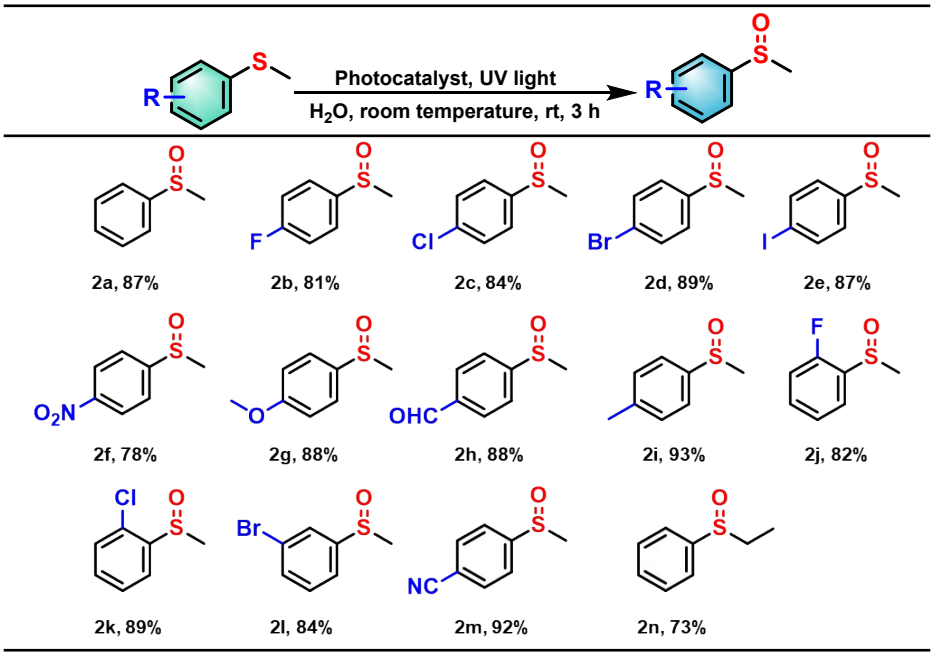

[a] Reaction conditions: thioanisole derivative (0.1 mmol, 1 equiv.), **PyCEPt⊃G**-ESY-SR101 assembly solution (1 mol%, 2 mL). 6 W UV light, room temperature, 3 h; [b] Isolated yields.

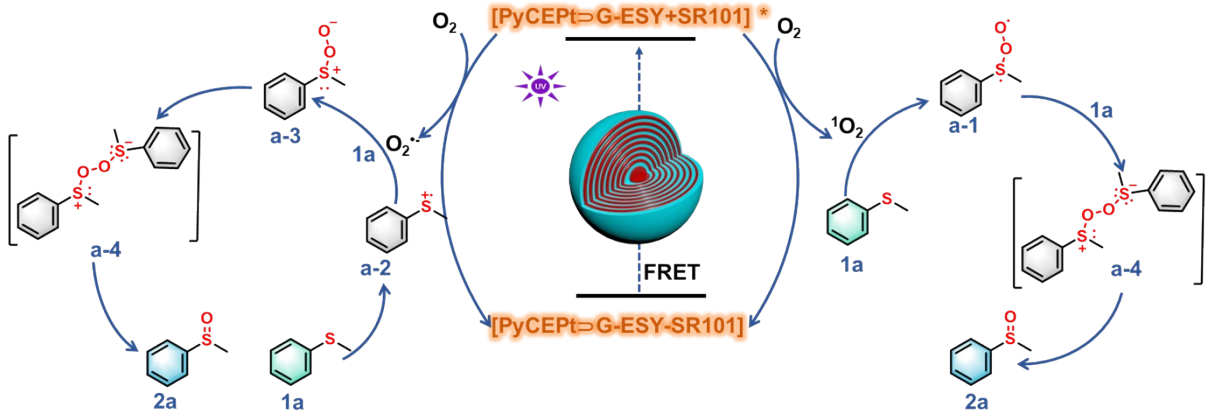

Fig. S58 The plausible mechanism for photooxidation reaction of thioanisole.

Thioanisole (0.1 mmol, 1 equiv.) and **PyCEPt⊃G**-ESY-SR101 assembly solution (1.0 mol%, 2 mL) were added to a vial. The reaction mixture was subsequently subjected to irradiation with a 6 W, 365 nm UV light for 3 hours at room temperature. After that, it was extracted with DCM three times, the solvent was evaporated under reduced pressure, and was separated by column chromatography to obtain the product.

2a. 87% yield; ^{1}H NMR (400 MHz, $CDCl_3$, 298 K) δ 7.68 – 7.62 (m, 2H), 7.56 – 7.48 (m, 3H), 2.73 (s, 3H).

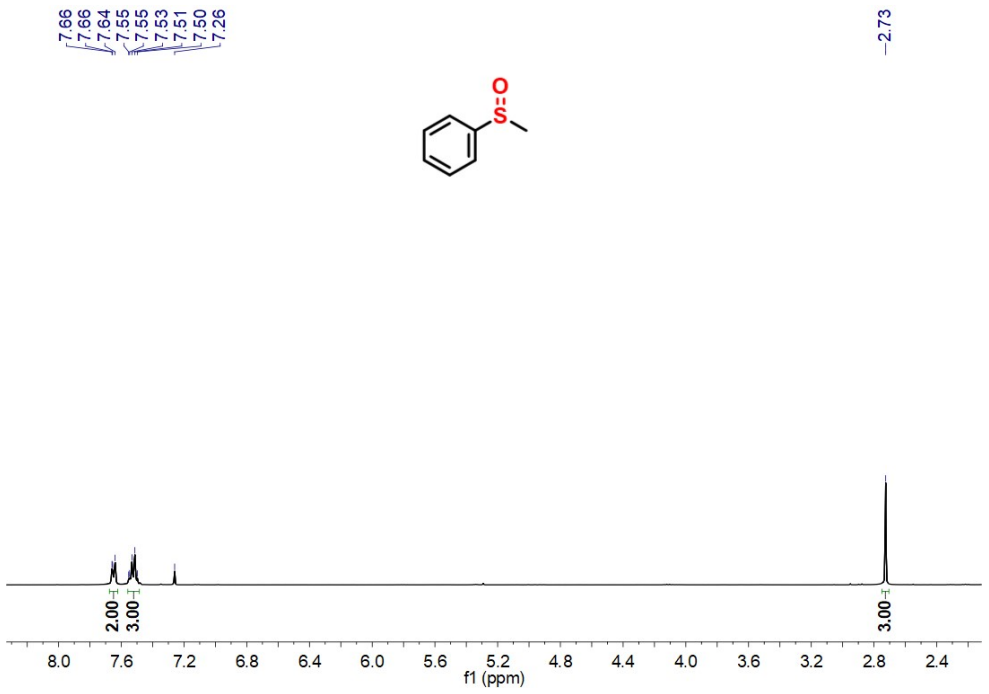

Fig. S59 ^{1}H NMR spectrum (400 MHz, $CDCl_3$, 298 K) of compound **2a**.

2b. 81% yield; ^{1}H NMR (400 MHz, $CDCl_3$, 298 K) δ 7.66 (dd, J = 8.7, 5.1 Hz, 2H), 7.22 (d, J = 8.5 Hz, 2H), 2.72 (s, 3H).

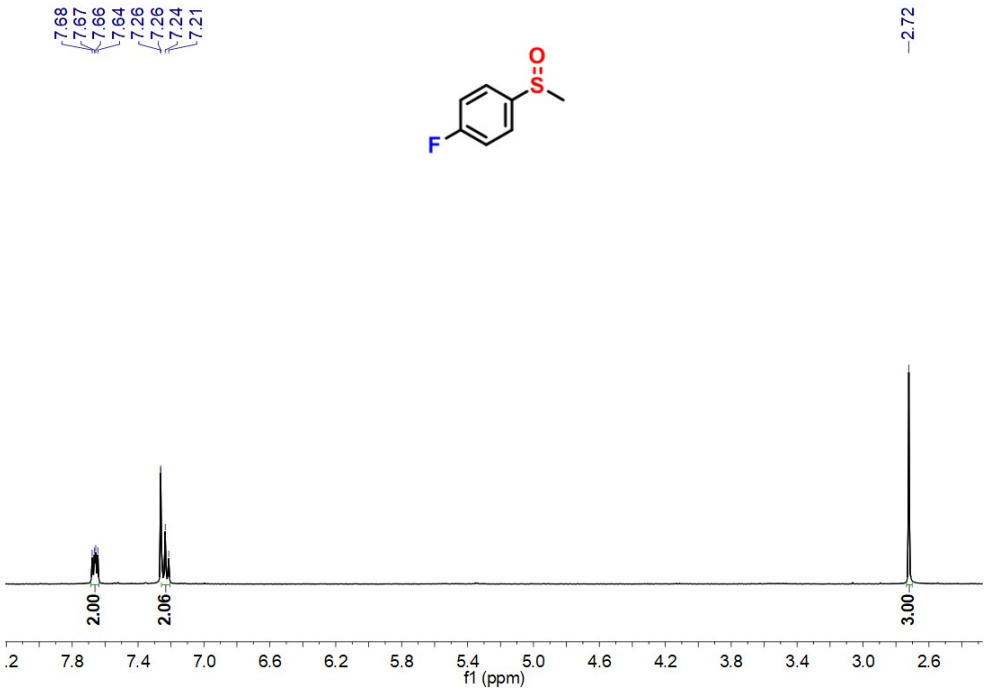

Fig. S60 ^{1}H NMR spectrum (400 MHz, $CDCl_3$, 298 K) of compound **2b**.

2c. 84% yield; ^{1}H NMR (400 MHz, $CDCl_3$, 298 K) δ 7.59 (d, J = 7.1 Hz, 2H), 7.51 (d, J = 7.0 Hz, 2H), 2.72 (s, 3H).

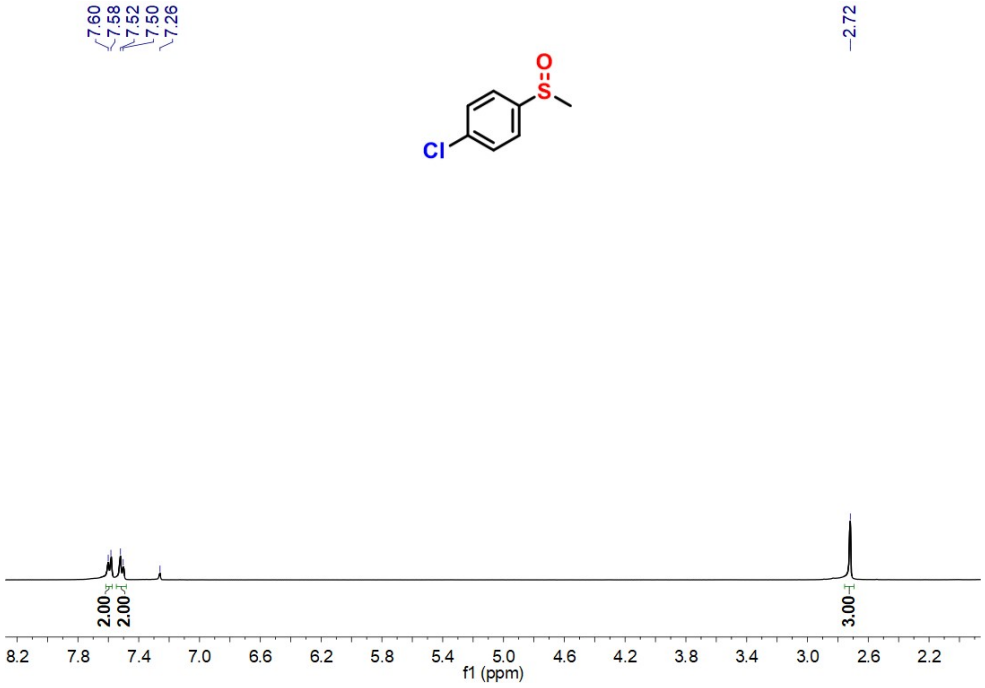

Fig. S61 ^{1}H NMR spectrum (400 MHz, $CDCl_3$, 298 K) of compound **2c**.

2d. 89% yield; ^{1}H NMR (400 MHz, $CDCl_3$, 298 K) δ 7.68 (d, J = 8.4 Hz, 3H), 7.53 (d, J = 8.4 Hz, 3H), 2.73 (s, 4H).

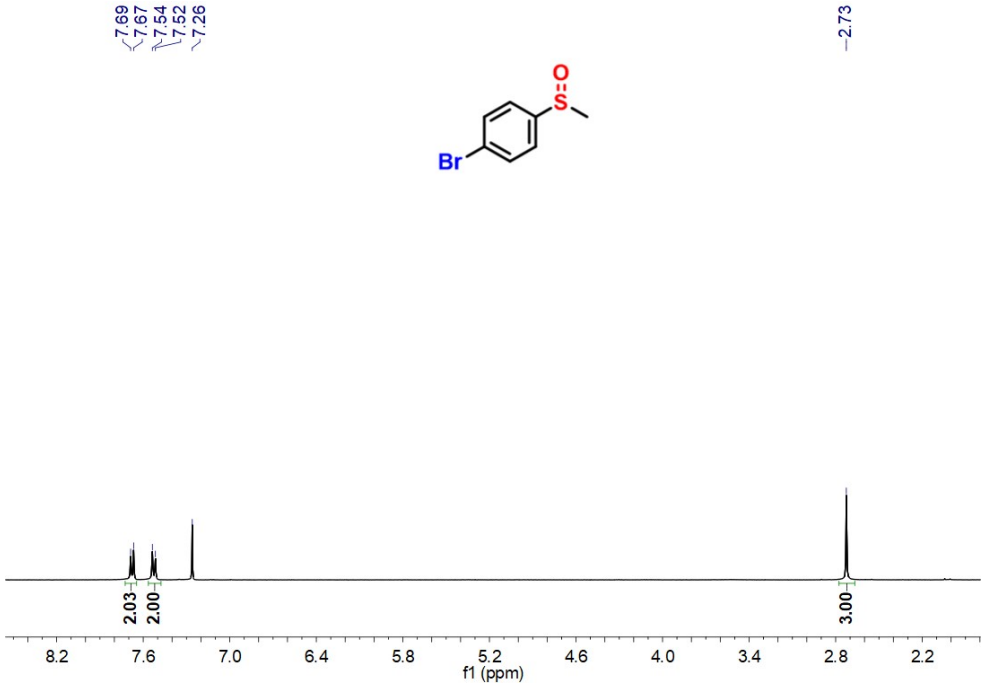

Fig. S62 ^{1}H NMR spectrum (400 MHz, $CDCl_3$, 298 K) of compound **2d**.

2e. 87% yield; ^{1}H NMR (400 MHz, $CDCl_3$, 298 K) δ 7.88 (d, J = 8.3 Hz, 2H), 7.38 (d, J = 8.3 Hz, 2H), 2.72 (s, 3H).

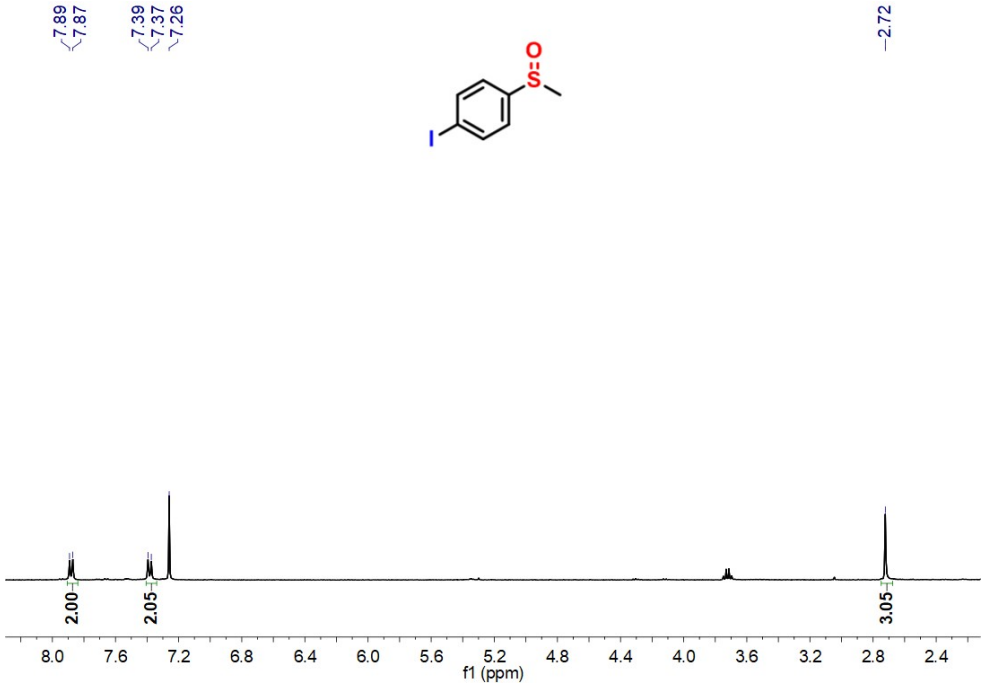

Fig. S63 ^{1}H NMR spectrum (400 MHz, $CDCl_3$, 298 K) of compound **2e**.

2f. 78% yield; ^{1}H NMR (400 MHz, $CDCl_3$, 298 K) δ 8.40 (d, J = 8.7 Hz, 3H), 7.84 (d, J = 8.7 Hz, 3H), 2.80 (s, 4H).

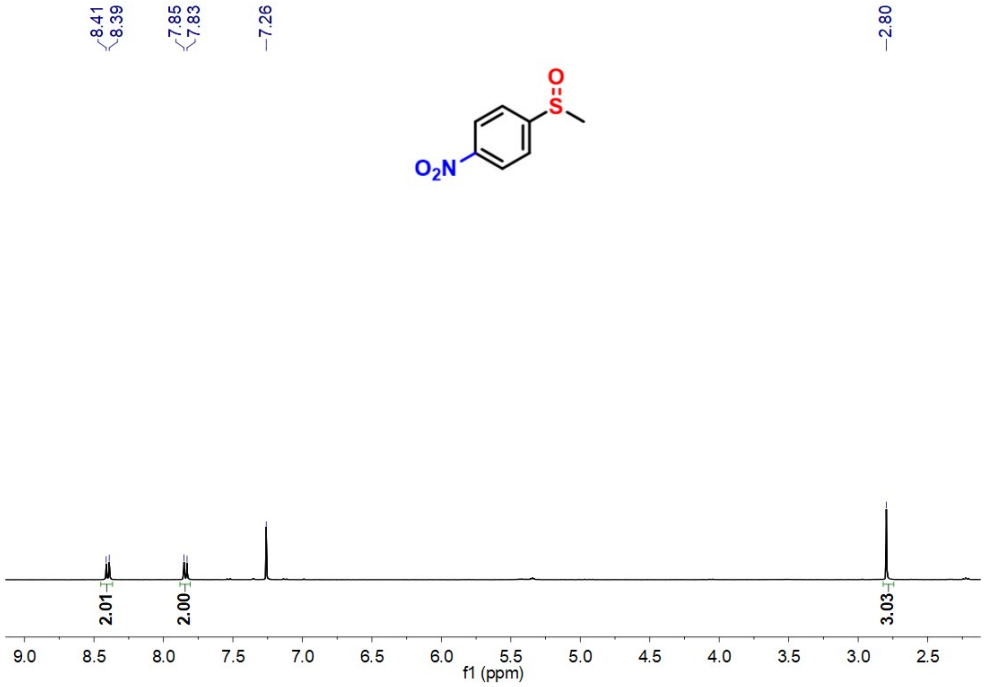

Fig. S64 ^{1}H NMR spectrum (400 MHz, $CDCl_3$, 298 K) of compound **2f**.

2g. 88% yield; ^{1}H NMR (400 MHz, $CDCl_3$, 298 K) δ 7.60 (d, J = 8.8 Hz, 3H), 7.03 (d, J = 8.8 Hz, 3H), 3.86 (s, 4H), 2.70 (s, 4H).

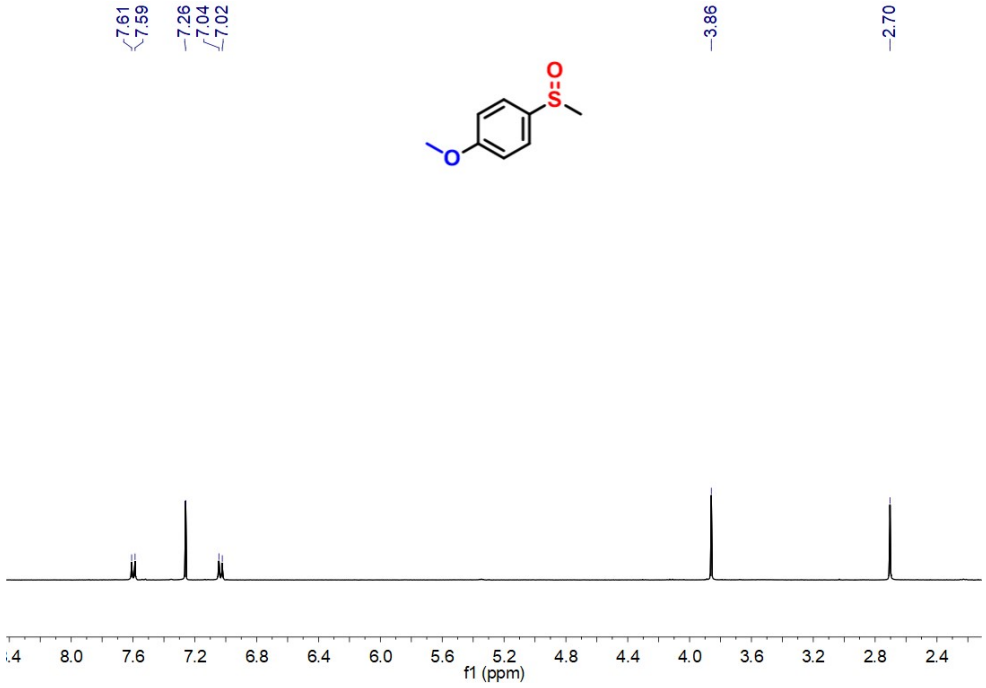

Fig. S65 ^{1}H NMR spectrum (400 MHz, $CDCl_3$, 298 K) of compound **2g**.

2h. 88% yield; ^{1}H NMR (400 MHz, $CDCl_3$, 298 K) δ 10.09 (s, 1H), 8.05 (d, J = 8.2 Hz, 2H), 7.82 (d, J = 8.2 Hz, 2H), 2.78 (s, 3H).

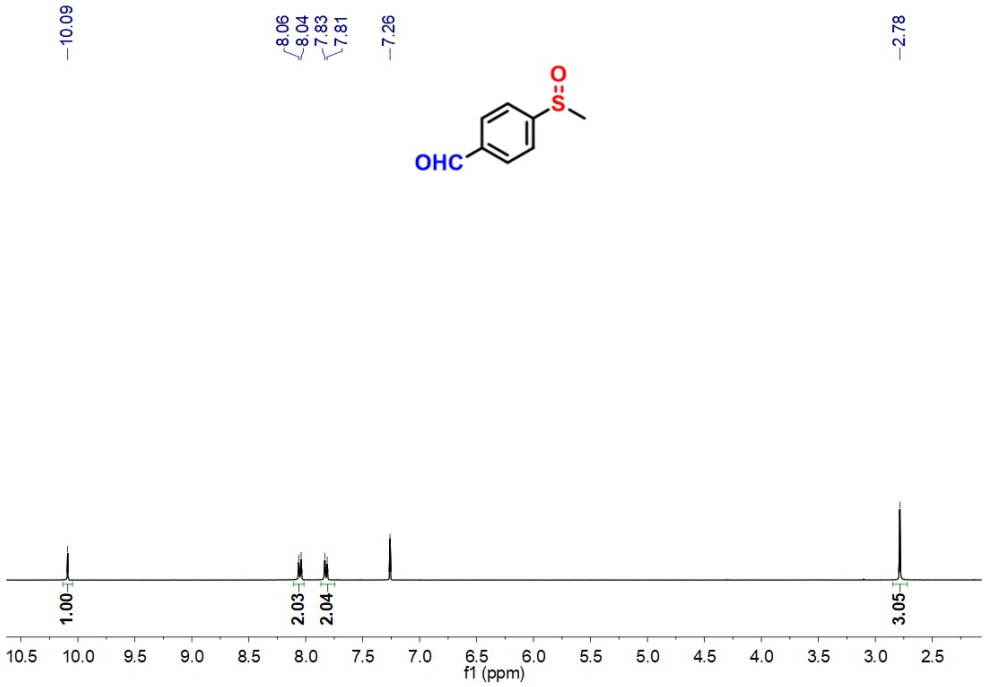

Fig. S66 ^{1}H NMR spectrum (400 MHz, $CDCl_3$, 298 K) of compound **2i**.

2i. 93% yield; ^{1}H NMR (400 MHz, $CDCl_3$, 298 K) δ 7.54 (d, J = 8.2 Hz, 2H), 7.33 (d, J = 7.9 Hz, 2H), 2.71 (s, 3H), 2.42 (s, 3H).

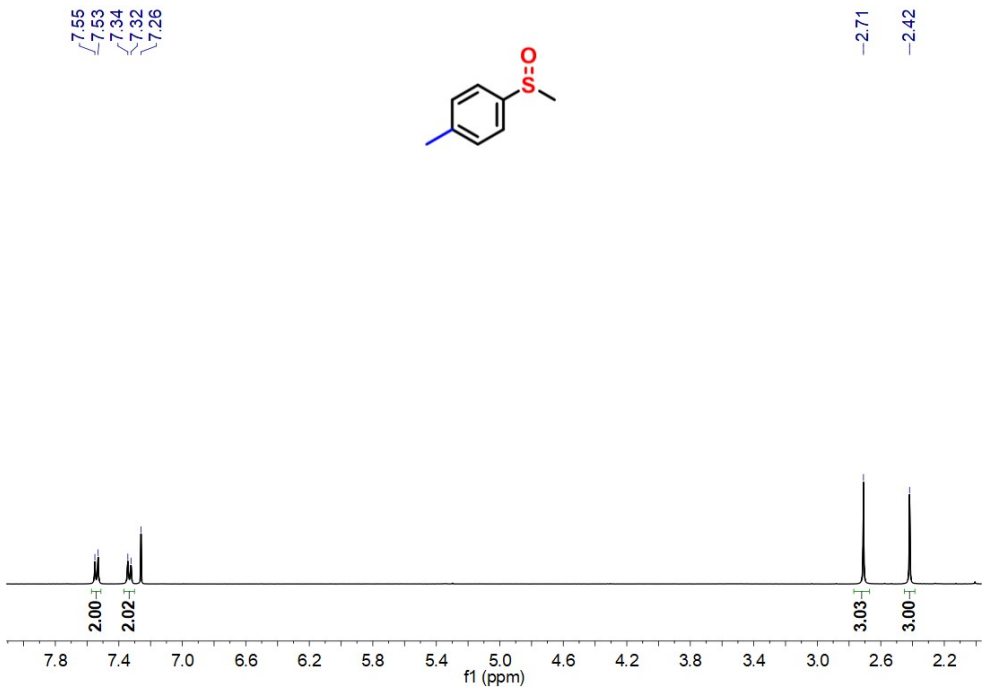

Fig. S67 ^{1}H NMR spectrum (400 MHz, $CDCl_3$, 298 K) of compound **2i**.

2j. 82% yield; ^{1}H NMR (400 MHz, $CDCl_3$, 298 K) δ 7.90 – 7.84 (m, 1H), 7.50 (ddd, J = 7.3, 6.3, 1.8 Hz, 1H), 7.40 (t, J = 7.6 Hz, 1H), 7.11 (d, J = 8.5 Hz, 1H), 2.84 (s, 3H).

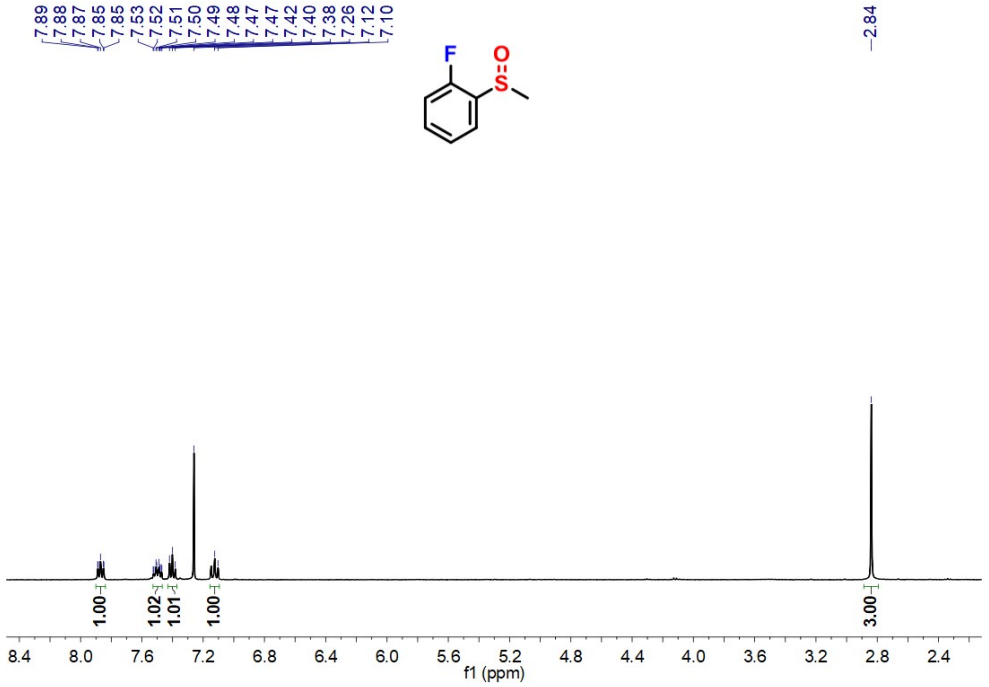

Fig. S68 ^{1}H NMR spectrum (400 MHz, $CDCl_3$, 298 K) of compound **2j**.

2k. 89% yield; ^{1}H NMR (400 MHz, $CDCl_3$, 298 K) δ 7.96 (dd, J = 7.8, 1.4 Hz, 1H), 7.54 (td, J = 7.6, 1.2 Hz, 1H), 7.47 – 7.42 (m, 1H), 7.41 – 7.37 (m, 1H), 2.82 (s, 3H).

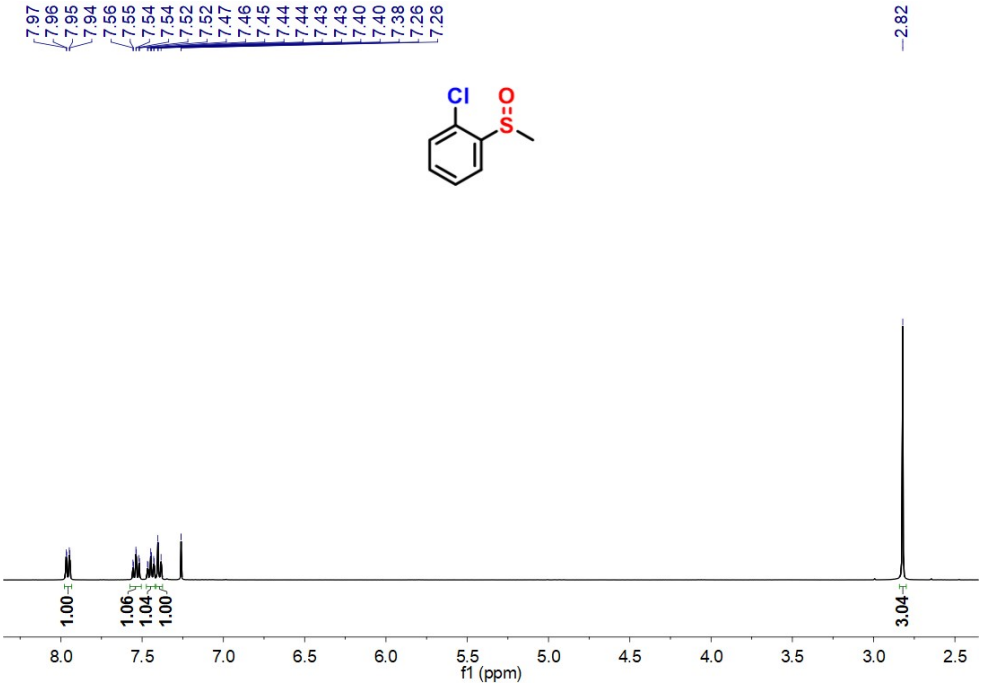

Fig. S69 ^{1}H NMR spectrum (400 MHz, $CDCl_3$, 298 K) of compound **2k**.

2l. 84% yield; ^{1}H NMR (400 MHz, $CDCl_3$, 298 K) δ 7.81 (s, 1H), 7.63 (d, J = 8.8 Hz, 1H), 7.55 (d, J = 7.8 Hz, 1H), 7.40 (t, J = 7.8 Hz, 1H), 2.75 (s, 3H).

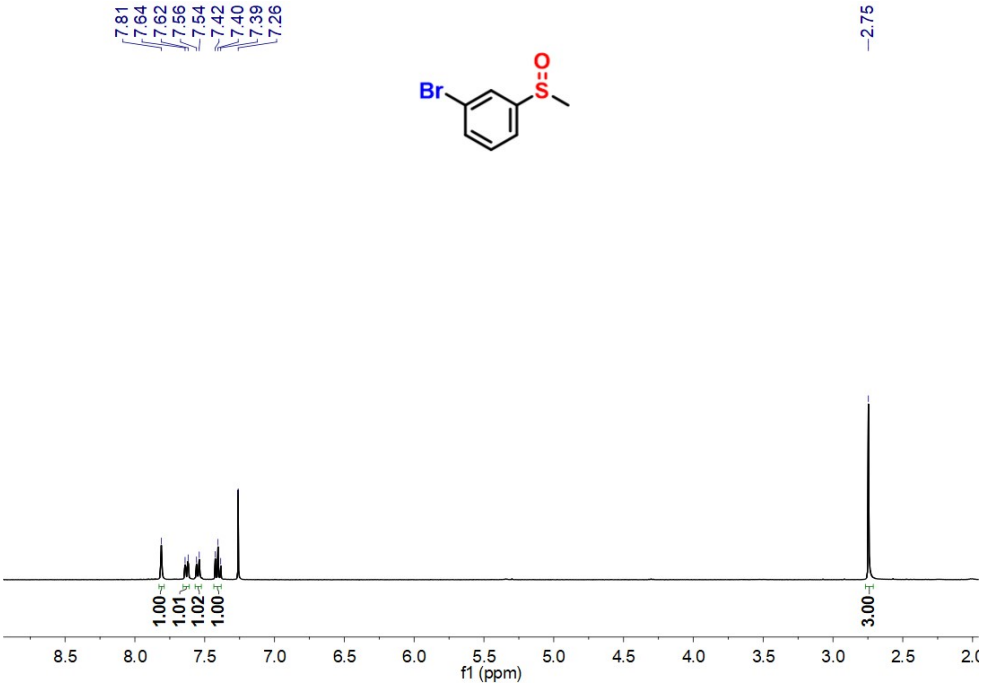

Fig. S70 ^{1}H NMR spectrum (400 MHz, $CDCl_3$, 298 K) of compound **2l**.

2m. 92% yield; ^{1}H NMR (400 MHz, $CDCl_3$, 298 K) δ 7.84 (d, J = 7.8 Hz, 2H), 7.77 (d, J = 7.8 Hz, 2H), 2.77 (s, 3H).

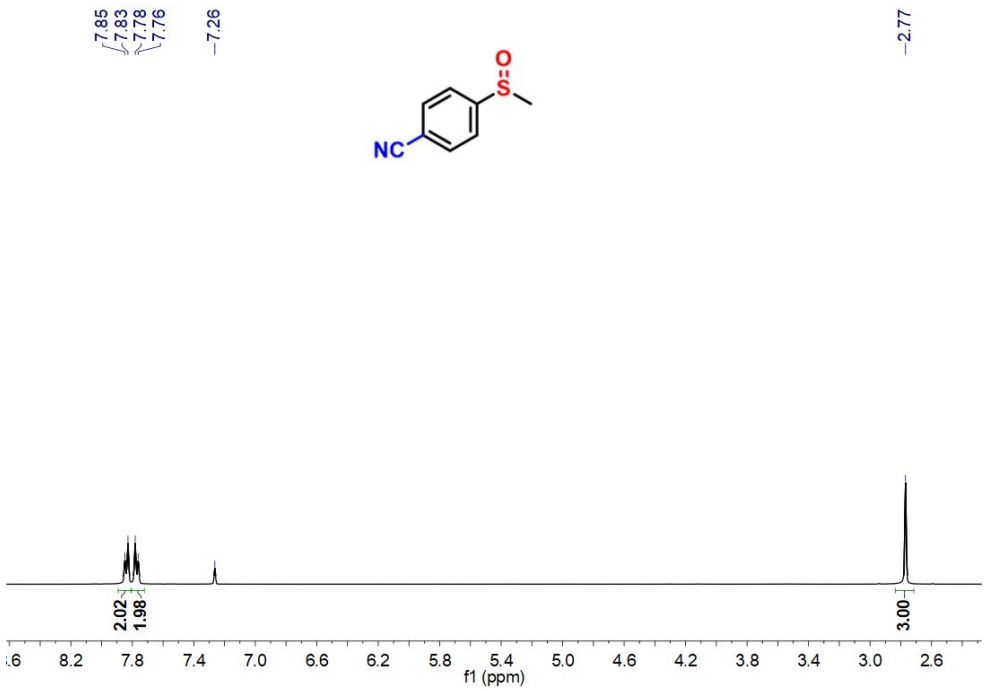

Fig. S71 ^{1}H NMR spectrum (400 MHz, $CDCl_3$, 298 K) of compound **2m**.

2n. 73% yield; ^{1}H NMR (400 MHz, $CDCl_3$, 298 K) δ 7.54 (d, J = 6.9 Hz, 2H), 7.45 (d, J = 6.5 Hz, 3H), 2.76 (m, 2H), 1.13 (t, J = 7.2 Hz, 3H).

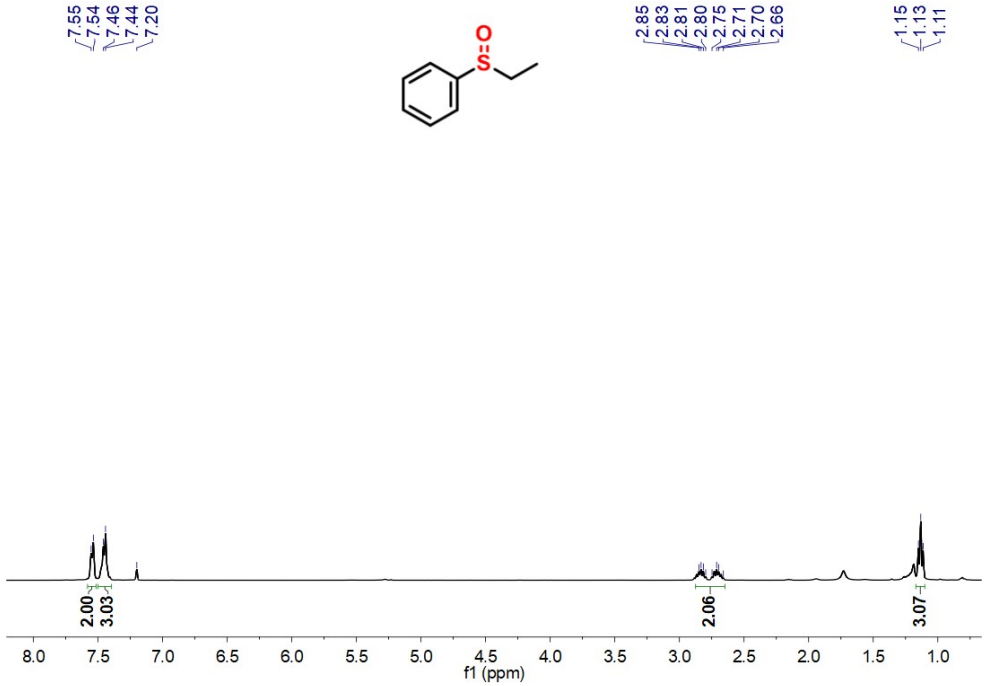

Fig. S72 ^{1}H NMR spectrum (400 MHz, $CDCl_3$, 298 K) of compound **2n**.

11. Reference

1 J. Huang, Y. Jiang, J. Yang, R. Tang, N. Xie, Q. Li, H. S. Kwok, B. Z. Tang and Z. Li, *J. Mater. Chem. C,* 2014, **2**, 2028.

2 T. Liargkova, N. Eleftheriadis, F. Dekker, E. Voulgari, C. Avgoustakis, M. Sagnou, B. Mavroidi, M. Pelecanou and D. Hadjipavlou-Litina, *Molecules,* 2019, **24**, 199.

3 W. Wang, Y. Zhang, B. Sun, L.-J. Chen, X.-D. Xu, M. Wang, X. Li, Y. Yu, W. Jiang and H.-B. Yang, *Chem. Sci.,* 2014, **5**, 4554.
4 X. Yan, M. Zhou, J. Chen, X. Chi, S. Dong, M. Zhang, X. Ding, Y. Yu, S. Shao and F. Huang, *Chem. Commun.,* 2011, **47**, 7086.
5 Z. Guo, J. Zhao, Y. Liu, G. Li, H. Wang, Y. Hou, M. Zhang, X. Li and X. Yan, *Chin. Chem. Lett.,* 2021, **32**, 1691.
6 X. Li, L. Wang, Y. Deng, Z. Luo, Q. Zhang, S. Dong and C. Han, *Chem. Commun.,* 2018, **54**, 12459.
7 J. Manna, C. J. Kuehl, J. A. Whiteford, P. J. Stang, D. C. Muddiman, S. A. Hofstadler and R. D. Smith, *J. Am. Chem. Soc.,* 1997, **119**, 11611.
8 M. Hao, G. Sun, M. Zuo, Z. Xu, Y. Chen, X.-Y. Hu and L. Wang, *Angew. Chem. Int. Ed.,* 2019, **59**, 10095.
9 P. K. Javvaji, A. Dhali, J. R. Francis, A. P. Kolte, A. Mech, S. C. Roy, A. Mishra and R. Bhatta, *Front. Cell Dev. Biol.,* 2020, **8**, 764.